Copy 175
RM A55E02

NACA RM A55E02

NACA

RESEARCH MEMORANDUM

THEORETICAL AND EXPERIMENTAL INVESTIGATION OF THE EFFECT OF YAW ON HEAT TRANSFER TO CIRCULAR CYLINDERS IN HYPERSONIC FLOW

By A. J. Eggers, Jr., C. Frederick Hansen,
and Bernard E. Cunningham

Ames Aeronautical Laboratory
Moffett Field, Calif.

CLASSIFIED DOCUMENT

NATIONAL ADVISORY COMMITTEE
FOR AERONAUTICS

WASHINGTON

July 25, 1955

NATIONAL ADVISORY COMMITTEE FOR AERONAUTICS

RESEARCH MEMORANDUM

THEORETICAL AND EXPERIMENTAL INVESTIGATION OF THE EFFECT OF YAW ON HEAT TRANSFER TO CIRCULAR CYLINDERS IN HYPERSONIC FLOW

By A. J. Eggers, Jr., C. Frederick Hansen,
and Bernard E. Cunningham

SUMMARY

An approximate theory is developed for predicting the rate of heat transfer to the stagnation region of blunt bodies in hypersonic flight. Attention is focused on the case where wall temperature is small compared to stagnation temperature. The effect of yaw on heat transfer to a cylindrical stagnation region is treated at some length, and it is predicted that large yaw should cause sizable reductions in heat-transfer rate.

Experiments were conducted in a so-called hypersonic gun tunnel to obtain a preliminary check on this theoretical prediction. These experiments consisted of measuring the rate of heat transfer to circular cylinders in a hypersonic air stream of nominal Mach number, 9.8, and nominal stagnation temperature, 2200° R. Experiment tended to confirm theory, showing, for example, that a 60-percent reduction in average heat-transfer rate can be obtained by yawing a circular cylinder 70° to the air stream.

INTRODUCTION

It has been suggested (see refs. 1 and 2) that blunting or rounding the leading edges of wings and bodies might substantially alleviate aerodynamic heating of these regions in hypersonic flight. There is, of course, the added advantage that round leading edges are structurally more practical than sharp leading edges, especially when the problem of absorbing heat is considered. Another consequence of round leading edges may be increased pressure drag. In the case of ballistic vehicles, this consequence is often an advantage (see ref. 1). In the case of glide vehicles, however, or more generally any vehicles required to operate for sustained periods in more or less level hypersonic flight, increased drag would most likely be viewed as a disadvantage.

Now, to be sure, rounding or blunting the nose of a body does not always increase drag. Indeed, small amounts of blunting may reduce the drag of a body (see, e.g., refs. 3 and 4). The same, however, cannot be said for blunting the leading edge of a wing. Even small blunting causes a sizable increase in drag. It is natural, then, to look for methods of minimizing this drag penalty, and the possibility of yawing or sweeping the leading edge comes to mind. Impact pressures should be, according to simple-sweep theory, decreased in proportion to the cosine squared of the angle of sweep; hence, as is intuitively obvious, large sweep should substantially reduce the drag penalty due to blunting. In view of this possibility it is important to inquire of the effect of yaw or sweep on heat transfer to a blunt leading edge.

A theoretical study of this effect was therefore undertaken, and the predictions of the theory were checked against the results of experiments carried out in a hot hypersonic air stream. The purpose of this report is to describe the problems and results of both the theoretical and experimental research.

SYMBOLS

$A,B,C,$ $D,E,F,$ $G, \ldots$	integration constants
C_b	specific heat of body material, ft-lb/slug $^{\circ}R$
C_p	specific heat at constant pressure, ft-lb/slug $^{\circ}R$
D_b	$2R_b$, twice the radius of curvature of the body at the stagnation point, ft
$f_1(t)$	$\dfrac{\int_o^t p\,dt}{p(t) - p(o)}$ parameter of time, sec
$f_2(t)$	$\dfrac{\int_o^t p_t\,dt}{p(t) - p(o)}$ parameter of time, sec
H	reservoir pressure, lb/ft^2 (unless otherwise specified)
h	specific enthalpy, ft-lb/slug
k	coefficient of thermal conductivity, ft-lb/ft-sec $^{\circ}R$
K	ratio of static pressure to pitot pressure, dimensionless

M	Mach number, dimensionless
n	exponent of temperature in thermal conductivity and viscosity functions (see eqs. (37) and (38)), dimensionless
Nu	Nusselt number based on a length D_b and stagnation temperature conditions, dimensionless
p	static pressure, lb/ft^2 (unless otherwise specified)
p_t	pitot pressure, lb/ft^2 (unless otherwise specified)
Pr	Prandtl number, dimensionless
q	dynamic pressure, lb/ft^2
R	gas constant, ft-lb/slug ^oR
R_b	radius of curvature of body at the stagnation point, ft
R_s	radius of curvature of the shock wave at the stagnation streamline, ft
Re	Reynolds number, based on twice the radius of curvature of the body at the stagnation point, dimensionless
$\bar{r},\theta,\varphi$	spherical coordinates, feet, degrees, and degrees, respectively
T	static temperature, ^oR
T_b	temperature of the body, ^oR
T_o	temperature at the interface, $x = 0$, with body at zero yaw, ^oR
$T_o(\lambda)$	temperature at the interface, $x = 0$, with body at angle of yaw λ, ^oR
T_r	recovery temperature, ^oR
T_t	stagnation temperature, ^oR
U_∞	stream velocity, ft/sec
u,v,w	velocity components in the x,y, and z directions, respectively, ft/sec
u,v	velocity components in the x and r directions, respectively, ft/sec

x,y,z Cartesian coordinates, ft

x,r cylindrical coordinates, ft

δ flow deflection angle, deg

ϵ dimensionless coordinate, $\frac{\bar{r} - R_b}{R_b}$ or $\frac{x_b - x}{R_b}$

γ ratio of specific heat at constant pressure to specific heat at constant volume, dimensionless

Γ $\left(\frac{1}{\gamma}\right)^{\frac{\gamma}{\gamma-1}} \left(\frac{\gamma+1}{2}\right)^{\frac{\gamma+1}{\gamma-1}}$, a function of γ, dimensionless

λ angle of yaw, deg

ρ density, slugs/cu ft

ρ_b density of the body material, slugs/cu ft

η $\int_0^T k\,dT$, a function of the coefficient of thermal conductivity and of temperature, ft-lb/ft-sec (unless otherwise specified)

σ acute angle of shock wave relative to stream velocity vector, deg

μ coefficient of viscosity, slugs/ft sec

μ_o coefficient of viscosity at temperature T_o, slugs/ft sec

$\mu_o(\lambda)$ coefficient of viscosity at temperature $T_o(\lambda)$, slugs/ft sec

τ time constant, sec

Subscripts

s conditions just behind shock wave on the stagnation streamline

b conditions at the stagnation point of the body

o conditions at the interface between regions 1 and 2 on the stagnation streamline (see sketch (a))

∞ conditions in the free stream

Superscripts

$'$ first derivative with respect to the x coordinate

$''$ second derivative with respect to the x coordinate

THEORY

General Equations in Cartesian Coordinates

The analysis proceeds from the equations of momentum, continuity, energy, and state for continuum fluid flow. The x, y, and z momentum equations are, respectively,

$$\rho \frac{\partial u}{\partial t} + \rho\left(u \frac{\partial u}{\partial x} + v \frac{\partial u}{\partial y} + w \frac{\partial u}{\partial z}\right) = - \frac{\partial p}{\partial x} - \frac{2}{3} \frac{\partial}{\partial x}\left[\mu\left(\frac{\partial u}{\partial x} + \frac{\partial v}{\partial y} + \frac{\partial w}{\partial z}\right)\right] + 2 \frac{\partial}{\partial x}\left(\mu \frac{\partial \mu}{\partial x}\right) + \frac{\partial}{\partial y}\left[\mu\left(\frac{\partial u}{\partial y} + \frac{\partial v}{\partial x}\right)\right] + \frac{\partial}{\partial z}\left[\mu\left(\frac{\partial u}{\partial z} + \frac{\partial w}{\partial x}\right)\right] \tag{1}$$

$$\rho \frac{\partial v}{\partial t} + \rho\left(u \frac{\partial v}{\partial x} + v \frac{\partial v}{\partial y} + w \frac{\partial v}{\partial z}\right) = - \frac{\partial p}{\partial y} - \frac{2}{3} \frac{\partial}{\partial y}\left[\mu\left(\frac{\partial u}{\partial x} + \frac{\partial v}{\partial y} + \frac{\partial w}{\partial z}\right)\right] + 2 \frac{\partial}{\partial y}\left(\mu \frac{\partial v}{\partial y}\right) + \frac{\partial}{\partial x}\left[\mu\left(\frac{\partial u}{\partial y} + \frac{\partial v}{\partial x}\right)\right] + \frac{\partial}{\partial z}\left[\mu\left(\frac{\partial v}{\partial z} + \frac{\partial w}{\partial y}\right)\right] \tag{2}$$

$$\rho \frac{\partial w}{\partial t} + \rho\left(u \frac{\partial w}{\partial x} + v \frac{\partial w}{\partial y} + w \frac{\partial w}{\partial z}\right) = - \frac{\partial p}{\partial z} - \frac{2}{3} \frac{\partial}{\partial z}\left[\mu\left(\frac{\partial u}{\partial x} + \frac{\partial v}{\partial y} + \frac{\partial w}{\partial z}\right)\right] +$$

$$2 \frac{\partial}{\partial z}\left(\mu \frac{\partial w}{\partial z}\right) + \frac{\partial}{\partial x}\left[\mu\left(\frac{\partial u}{\partial z} + \frac{\partial w}{\partial x}\right)\right] +$$

$$\frac{\partial}{\partial y}\left[\mu\left(\frac{\partial v}{\partial z} + \frac{\partial w}{\partial y}\right)\right] \tag{3}$$

The continuity equation is

$$\frac{\partial \rho}{\partial t} + \frac{\partial}{\partial x}(\rho u) + \frac{\partial}{\partial y}(\rho v) + \frac{\partial}{\partial z}(\rho w) = 0 \tag{4}$$

and the energy equation is

$$\rho\left(u \frac{\partial h}{\partial x} + v \frac{\partial h}{\partial y} + w \frac{\partial h}{\partial z} + \frac{\partial h}{\partial t}\right) - \left(\frac{\partial p}{\partial t} + u \frac{\partial p}{\partial x} + v \frac{\partial p}{\partial y} + w \frac{\partial p}{\partial z}\right)$$

$$= \frac{\partial}{\partial x}\left(k \frac{\partial T}{\partial x}\right) + \frac{\partial}{\partial y}\left(k \frac{\partial T}{\partial y}\right) + \frac{\partial}{\partial z}\left(k \frac{\partial T}{\partial z}\right) + \mu\left[2\left(\frac{\partial u}{\partial x}\right)^2 + 2\left(\frac{\partial v}{\partial y}\right)^2 +\right.$$

$$\left. 2\left(\frac{\partial w}{\partial z}\right)^2 + \left(\frac{\partial u}{\partial y} + \frac{\partial v}{\partial x}\right)^2 + \left(\frac{\partial u}{\partial z} + \frac{\partial w}{\partial x}\right)^2 + \left(\frac{\partial v}{\partial z} + \frac{\partial w}{\partial y}\right)^2 - \frac{2}{3}\left(\frac{\partial u}{\partial x} + \frac{\partial v}{\partial y} + \frac{\partial w}{\partial z}\right)^2\right] \tag{5}$$

while the equation of state is taken in the form

$$p = p(\rho, T) \tag{6}$$

Derivations of the momentum and energy equations are given in numerous sources (see, e.g., refs. 5, 6, and 7). Note that the coefficients of viscosity and thermal conductivity, and the heat capacity have been treated as variables. It is intended that by so doing a more accurate solution will be obtained for hypersonic flows with their characteristically large temperature and pressure gradients.

Let us now consider the particular flows of interest in this paper, namely, those in the region of a stagnation point.

Model of Flow and Method of Analysis

It is instructive in setting up the model to consider the qualitative aspects of temperature and velocity variations in the flow along the stagnation streamline. Restricting the analysis to steady hypersonic flow, that is $M_\infty \sin \delta >> 1$, we will assume that the surface temperature is low compared to the stagnation temperature of the air. This assumption seems quite reasonable since practical surface materials will probably be destroyed if surface temperatures are allowed to approach stagnation temperature. It will be assumed further that the Reynolds number of the flow is large enough so that heat conduction and viscous shearing in the shock process is distinct and separate from the corresponding phenomena occurring in the boundary layer adjacent to the surface of the body. Accordingly, temperature and velocity should vary along the stagnation streamline similar to the manner shown in sketch (a).

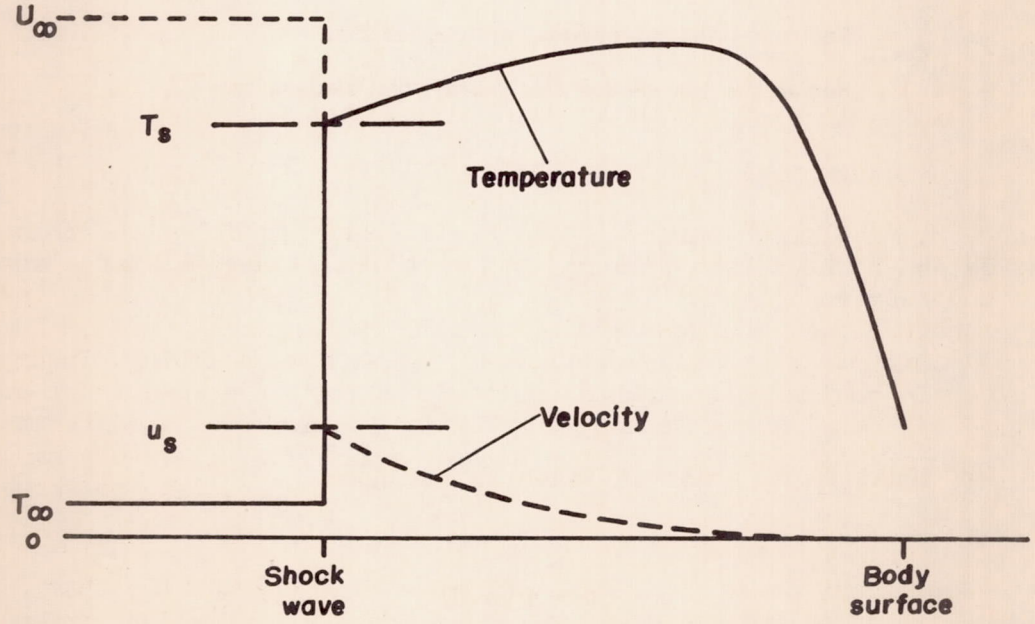

Sketch (a)

There is an abrupt and large increase in temperature and decrease in velocity of the air as it passes through the bow shock. Proceeding from the shock in the direction of the body, temperature continues to increase slowly while the velocity decreases slowly towards zero. Near the surface of the body, the air temperature ceases to increase and, in fact, begins to fall off steeply in the direction of the body temperature. The velocity of the flow must, of course, be close to zero in this region.

On the basis of these observations the following simplified model is proposed and employed throughout this study of heat transfer in a stagnation region.

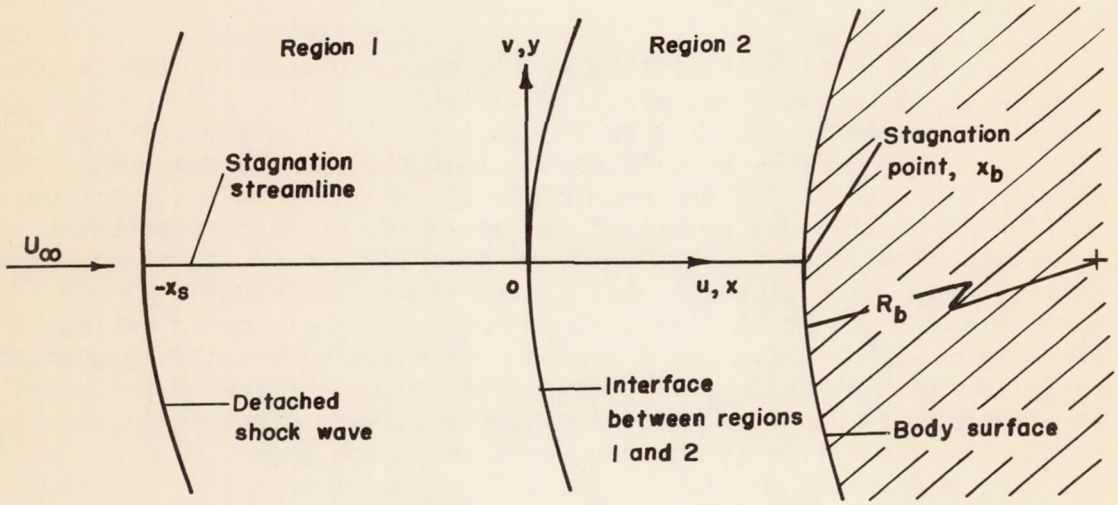

Region 1— Incompressible, nonviscous flow

Region 2— Low-velocity, compressible, viscous flow

Sketch (b)

Since M_∞ is large compared to 1, M_s is substantially less than 1 and the detached shock wave is located a relatively short distance ahead of the body surface (i.e., $(x_s + x_b)/R_b << 1$). The flow between the shock wave and the body surface is divided into two regions. Region 1 is taken as a domain of essentially nonviscous, non-heat-conducting, incompressible flow while region 2 is taken as a domain of very low speed, but compressible, viscous, and heat-conducting flow. It is anticipated further that in region 2 the u and v components of velocity will be very small. The component of velocity w due to yaw may, of course, take on rather large values.

Now it may be demonstrated with equations (1) and (2) that $\partial^2 p/\partial y^2$ becomes relatively independent of x along the stagnation streamline in

the limit as the disturbed flow extends only a short distance away from the body. Inasmuch as this is the type of flow of interest here, it will be assumed throughout this analysis that $\partial^2 p/\partial y^2$ is essentially constant along the stagnation streamline between the shock and the body.

With these assumptions, the derivative with respect to y of the y momentum equation yields a differential equation that becomes tractable, both in regions 1 and 2, when terms that vanish in the neighborhood of the stagnation streamline are dropped. Approximate solutions to these simplified y momentum equations are found for the u velocity along the stagnation streamline in region 1, and for the derivative of this velocity along the stagnation streamline in region 2. The constants appearing in these solutions are determined by matching the boundary conditions at the shock wave and at the surface of the body, and by matching flow conditions at the interface. This procedure fixes the locations of the shock wave and interface relative to the body.

The energy equation is simplified in an analogous manner, and solutions valid in the neighborhood of the stagnation streamline are found for regions 1 and 2. The rate of heat transfer per unit area to the stagnation region of the body follows from the solution to the energy equation for region 2.

Let us see how these thoughts apply in the case of a two-dimensional stagnation region.

Heat Transfer to a Cylindrical Stagnation Region

Zero yaw.- This problem has been treated for incompressible flow by Howarth (ref. 7) and more recently for the compressible flow by Cohen and Reshotko (ref. 8). One reason for re-investigating the matter here is to obtain compressible flow solutions which can be extended with relative ease to the case of a yawed cylinder. In addition it was desired to obtain solutions which may be better suited to account for real gas effects, such as dissociation.

To proceed, then, the stagnation streamlines are taken to lie in the x-z plane. The origin of the coordinate system is at the interface between regions 1 and 2, and the shock-wave and body-surface locations in this plane are x_s and x_b, respectively (see sketch (a)). For the case of zero yaw, the z component of velocity and all derivatives with respect to z are, of course, identically zero.

First a solution will be found to the steady-state y momentum equation near the stagnation streamline in region 1. Since the flow is assumed incompressible and nonviscous in this region, equation (2)

simplifies to

$$u \frac{\partial v}{\partial x} + v \frac{\partial v}{\partial y} = - \frac{1}{\rho} \frac{\partial p}{\partial y} \tag{7}$$

Differentiating equation (7) with respect to y there is obtained

$$u \frac{\partial}{\partial y}\left(\frac{\partial v}{\partial x}\right) + \frac{\partial u}{\partial y} \frac{\partial v}{\partial x} + \left(\frac{\partial v}{\partial y}\right)^2 + v \frac{\partial^2 v}{\partial y^2} = - \frac{1}{\rho} \frac{\partial^2 p}{\partial y^2} \tag{8}$$

On the stagnation streamline v is identically zero and, therefore, $\partial v/\partial x$ is also zero. In addition, the continuity equation (eq. (4)) becomes, for incompressible, two-dimensional flow

$$\frac{\partial u}{\partial x} + \frac{\partial v}{\partial y} = 0 \tag{9}$$

Using this information with equation (8), one obtains

$$-u \frac{\partial^2 u}{\partial x^2} + \left(\frac{\partial u}{\partial x}\right)^2 = - \frac{1}{\rho} \frac{\partial^2 p}{\partial y^2} \tag{10}$$

Treating $\partial^2 p/\partial y^2$ as a function of y only, and noting that equation (10) becomes a total differential equation along a line y = constant, yields a general solution for velocity along the stagnation streamline

$$u = Ae^{Cx} + Be^{-Cx} \tag{11}$$

where the constants A, B, and C are related by

$$4ABC^2 = \frac{1}{\rho} \frac{\partial^2 p}{\partial y^2} \tag{12}$$

Note that the constants may be real or imaginary, depending on the boundary conditions.

Now it is anticipated that the velocity u will very nearly vanish at the interface $x = 0$ (i.e., in the sense that $u_o/u_s << 1$); hence B will be approximately $-A$, and the corresponding approximate solution for velocity is[1]

$$u = 2A \sinh Cx \tag{13}$$

To the same order of approximation, the second derivative of velocity at the interface, u_o'', also vanishes. The product $2AC$ is just the velocity derivative at the interface and can be evaluated from equations (10) and (13), thus

$$2AC = u_o' = \pm \sqrt{-\frac{1}{\rho} \frac{\partial^2 p}{\partial y^2}} \tag{14}$$

Note that the negative root correctly describes the flow in the coordinate system of sketch (b), since velocity decreases with increasing x.

Consider next the steady-state y momentum equation near the stagnation streamline in region 2. In this domain viscous terms must, of course, be retained and thus the derivative of equation (2) with respect to y yields

$$\rho u \frac{\partial^2 v}{\partial x \partial y} + u \frac{\partial \rho}{\partial y} \frac{\partial v}{\partial x} + \rho \frac{\partial v}{\partial x} \frac{\partial u}{\partial y} + \rho v \frac{\partial^2 v}{\partial y^2} + v \frac{\partial \rho}{\partial y} \frac{\partial v}{\partial y} + \rho \left(\frac{\partial v}{\partial y} \right)^2$$

$$= - \frac{\partial^2 p}{\partial y^2} - \frac{2}{3} \frac{\partial^2}{\partial y^2} \left[\mu \left(\frac{\partial u}{\partial x} + \frac{\partial v}{\partial y} \right) \right] + 2 \frac{\partial^2}{\partial y^2} \left(\mu \frac{\partial v}{\partial y} \right) + \frac{\partial^2}{\partial y \partial x} \left[\mu \left(\frac{\partial u}{\partial y} + \frac{\partial v}{\partial x} \right) \right] \tag{15}$$

Now close to the surface of the body the left-hand side of this expression is negligible and the right-hand side simplifies so that the equation may be written (see Appendix A)

$$\frac{\partial}{\partial x} \left(\mu \frac{\partial^2 u}{\partial x^2} \right) = - \frac{\partial^2 p}{\partial y^2} \tag{16}$$

---

[1]In the limit of zero boundary-layer thickness, this solution is exactly the one to which equation (11) reduces.

Along the stagnation streamline this equation integrates to

$$\mu \frac{\partial^2 u}{\partial x^2} = - \frac{\partial^2 p}{\partial y^2} x + D \tag{17}$$

The constant D is zero since $\partial^2 u/\partial x^2 = u_o'' = 0$ at the interface ($x = 0$). Near the surface of the body, equation (17) can be integrated to obtain

$$\mu \frac{\partial u}{\partial x} = - \frac{\partial^2 p}{\partial y^2} \frac{x^2}{2} + \mu_o u_o' \tag{18}$$

In order to satisfy the boundary condition at the body surface $\left(\frac{\partial v}{\partial y}\right)_b = \left(\frac{\partial u}{\partial x}\right)_b = 0$, it follows from equations (18) and (14) that

$$x_b^2 = \frac{2\mu_o}{\sqrt{-\rho \frac{\partial^2 p}{\partial y^2}}} \tag{19}$$

Now ρ and $\partial^2 p/\partial y^2$ can be evaluated at the shock wave since both are considered constant throughout region 1. In Appendix B it is demonstrated that for two-dimensional flow

$$\left(\rho \frac{\partial^2 p}{\partial y^2}\right)_s = - \frac{6\rho_\infty^2 U_\infty^2}{(\gamma_s - 1)R_s^2} \tag{20}$$

where R_s is the radius of curvature of the shock wave in the stagnation region. Substituting equation (20) in equation (19) we obtain

$$\frac{x_b}{R_b} = \left(\frac{\gamma_s - 1}{6}\right)^{1/4} \left(\frac{\mu_o}{\mu_\infty} \frac{R_s}{R_b}\right)^{1/2} \frac{2}{Re_\infty^{1/2}} \tag{21}$$

where Re_∞ is the free-stream Reynolds number based on D_b, twice the radius of curvature of the body at the stagnation point. Note also that the effective value of γ, the ratio of specific heats, at the shock wave is allowed to vary from the free-stream value. In this way, changes in internal molecular energy which are manifest at the high temperatures encountered in hypersonic flight can be considered.

There remains the problem of solving the energy equation. In region 1, the energy equation is simplified by neglecting all the viscous and heat-conduction terms. Then, for the two-dimensional problem considered here, equation (5) reduces to

$$u \frac{\partial u}{\partial x} + C_p \frac{\partial T}{\partial x} = 0 \tag{22}$$

for which the solution is

$$\int_T^{T_t} C_p dT = \frac{u^2}{2} \tag{23}$$

It can be seen from equation (23) that the interface temperature T_o is approximately the stagnation temperature T_t, since the velocity at the interface nearly vanishes. The stagnation temperature is, of course, given by the integral equation

$$\int_{T_\infty}^{T_t} C_p dT = \frac{\gamma_\infty R T_\infty M_\infty^2}{2} \tag{24}$$

where for very high velocity flow the lower limit of the integral will be neglected.

Next consider the energy equation in region 2. Proceeding in a manner analogous to that used in studying the y momentum equation in this region, we neglect the terms with the factors u, v, $\partial u/\partial x$, and $\partial v/\partial y$. Thus equation (5) becomes simply the heat-conduction equation

$$\frac{\partial}{\partial x}\left(k \frac{\partial T}{\partial x}\right) + \frac{\partial}{\partial y}\left(k \frac{\partial T}{\partial y}\right) = 0 \tag{25}$$

The coefficient of thermal conductivity, k, is considered a known function of temperature (pressure is essentially constant). Thus a new function of temperature, η, may be defined such that

$$\eta = \int_o^T k \, dT \tag{26}$$

Then equation (25) may be expressed in terms of the function η

$$\frac{\partial^2 \eta}{\partial x^2} + \frac{\partial^2 \eta}{\partial y^2} = 0 \tag{27}$$

Inasmuch as the body boundary is cylindrical, it is convenient to use the general solution to equation (27) in terms of the polar coordinates $(\bar{r}, \theta)$. Thus

$$\eta = A + B \ln \bar{r} + \sum_{n=1}^{\infty} \left[\left(C_n \bar{r}^n + \frac{D_n}{\bar{r}^n} \right) \cos n\theta + \left(E_n \bar{r}^n + \frac{F_n}{\bar{r}^n} \right) \sin n\theta \right] \tag{28}$$

The origin of the coordinate system is now taken as the center of curvature of the body, and θ as the acute angle between the radius vector $\bar{r}$ and the stagnation streamline. If a surface temperature is assumed independent of the angle θ,[2] the solution on the stagnation streamline $(\theta = 0)$ reduces to

$$\eta = \eta_b + B \ln \frac{\bar{r}}{R_b} + \sum_{n=1}^{\infty} C_n \bar{r}^n \left[1 - \left(\frac{R_b}{\bar{r}} \right)^{2n} \right] \tag{29}$$

Letting $\frac{\bar{r}}{R_b} = 1 + \epsilon$, where ϵ is very small compared to unity, and expanding equation (29) in a series of ascending powers of ϵ, we obtain

$$\eta = \eta_b + G \left(\epsilon - \frac{\epsilon^2}{2} \right) + O(\epsilon^3) \tag{30}$$

where G is the constant $\left(B + \sum_{n=1}^{\infty} 2nR_b{}^n C_n \right)$. It is indicated by this equation that η varies essentially linearly with ϵ, since $\epsilon^2/2$ is negligible compared to ϵ and terms of higher order in ϵ should be very small indeed.[3] Since $\epsilon = (x_b - x)/R_b << 1$, equation (30) can be written

$$\eta = \eta_o - (\eta_o - \eta_b) \frac{x}{x_b} \tag{31}$$

---

[2]The dependence of surface temperature on θ should be small in the stagnation region.

[3]It should be pointed out that this argument hinges implicitly on the assumption that η is a weak function of θ near the stagnation streamline.

According to this expression, the rate of heat transfer per unit area to the stagnation region of the body is

$$-\eta_b' = \frac{\eta_o - \eta_b}{x_b} = \frac{1}{x_b} \int_{T_b}^{T_o} k \, dT \tag{32}$$

The stagnation-line coordinate x_b is substituted from equation (21), and the rate of heat transfer becomes

$$-\eta_b' = \left[\frac{3}{8(\gamma_s - 1)}\right]^{1/4} \left(\frac{\mu_\infty}{\mu_o} \frac{R_b}{R_s}\right)^{1/2} \frac{Re_\infty^{1/2}}{R_b} \int_{T_b}^{T_o} k \, dT \tag{33}$$

A Nusselt number is defined for interface temperature conditions using a characteristic length equal to twice the radius of curvature of the body and a temperature potential of $(T_o - T_b)$; thus

$$Nu = - \frac{2\eta_b' R_b}{k_o(T_o - T_b)} \tag{34}$$

or, substituting from equation (33) into (34)

$$Nu = \left(\frac{6}{\gamma_s - 1}\right)^{1/4} \left(\frac{\mu_\infty}{\mu_o} \frac{R_b}{R_s}\right)^{1/2} \frac{Re_\infty^{1/2}}{k_o(T_o - T_b)} \int_{T_b}^{T_o} k \, dT \tag{35}$$

For a relatively cool body in hypersonic flight, it is possible to disregard the lower limit of the integral and the value of body temperature T_b compared to the interface temperature T_o.

Note that the solutions given by equations (33) and (35) can be used for the case where viscosity, thermal conductivity, and specific heat are arbitrary functions of temperature. For instance, these functions can be calculated to include the effects of vibrational and dissociational molecular energy if the extent to which these energy modes are excited is known throughout the flow. It is sufficient for the most part in this paper to consider the specific heat a constant and the viscosity and thermal

conductivity as proportional to the nth power of temperature. In this case from equation (24) $\left(\text{note } \frac{T_o}{T_t} \approx 1, \frac{T_o}{T_\infty} >> 1\right)$

$$\frac{T_o}{T_\infty} = \left(\frac{\gamma_\infty R}{2C_p}\right) M_\infty^2 \tag{36}$$

Noting that

$$\frac{1}{k_o(T_o - T_b)} \int_{T_b}^{T_o} k\, dT = \frac{1}{T_o - T_b} \int_{T_b}^{T_o} \left(\frac{T}{T_o}\right)^n dT = \frac{1}{n+1} \frac{1 - \left(T_b/T_o\right)^{n+1}}{1 - T_b/T_o} \tag{37}$$

and that

$$\left(\frac{\mu_\infty}{\mu_o}\right)^{1/2} = \left(\frac{T_\infty}{T_o}\right)^{n/2} = \left(\frac{2C_p}{\gamma_\infty R}\right)^{n/2} M_\infty{}^{-n} \tag{38}$$

it is seen that the expression for Nusselt number (eq. (35)) becomes

$$Nu = \frac{1}{n+1} \left(\frac{6}{\gamma_s - 1}\right)^{1/4} \left(\frac{R_b}{R_s}\right)^{1/2} \left(\frac{2C_p}{\gamma_\infty R}\right)^{n/2} \frac{Re_\infty{}^{1/2}}{M_\infty{}^n} \frac{1 - \left(T_b/T_o\right)^{n+1}}{1 - (T_b/T_o)} \tag{39}$$

and the rate of heat transfer per unit area to the stagnation region of the body is, in terms of free-stream conditions,

$$-\eta_b{}' = \left(\frac{k_\infty T_\infty}{R_b}\right) \left[\frac{3}{8(\gamma_s - 1)}\right]^{1/4} \left(\frac{R_b}{R_s}\right)^{1/2} \left(\frac{\gamma_\infty R}{2C_p}\right)^{\frac{n}{2}+1} \frac{Re_\infty{}^{1/2} M_\infty{}^{n+2}}{n+1} \left[1 - \left(\frac{T_b}{T_o}\right)^{n+1}\right] \tag{40}$$

These considerations complete the zero-yaw analysis. However, before undertaking the study of effects of yaw on heat transfer it is appropriate to make a few remarks. By way of introduction it should be pointed out that a procedure quite analogous to that just described for treating a cylindrical stagnation region can be employed to treat an axially symmetric

stagnation region. The results of such an analysis are presented in Appendix C. There is then the general question of the legitimacy of the several assumptions underlying the present treatment of stagnation-point flows. In order to shed some light on this matter it was undertaken in Appendix D to examine the solutions obtained to see whether they are consistent with these assumptions and with pertinent results obtained by others. In this regard it is shown that the presumption of a constant second derivative of pressure normal to the stagnation streamline yields solutions for the distance between shock wave and body which are quite close to observed values. Next, it is demonstrated that, as assumed, the velocity u is negligibly small throughout region 2 under continuum flow conditions. Then it is shown that the largest of the viscous dissipation terms neglected in the energy equation for region 2 is indeed small compared to the heat-conduction terms. It is found too that the analysis predicts an amount of heat convected into region 2 which is the proper order of magnitude to account for the heat transferred to the body. Finally, it is shown that under comparable conditions equation (35) of this paper predicts essentially the same heat transfer as references 7 and 8.

In view of these results it would seem that the simplified analysis presented here for stagnation-region flows is, while on the one hand certainly approximate, on the other hand quite capable of predicting useful information. Accordingly, we proceed to the study of effects of yaw on heat transfer.

Yaw.- In this case the x direction is normal to and the z direction is parallel to the stagnation line of the body (see plan view, sketch (c)). Then the z component of velocity has a finite value, but all z derivatives are again zero.

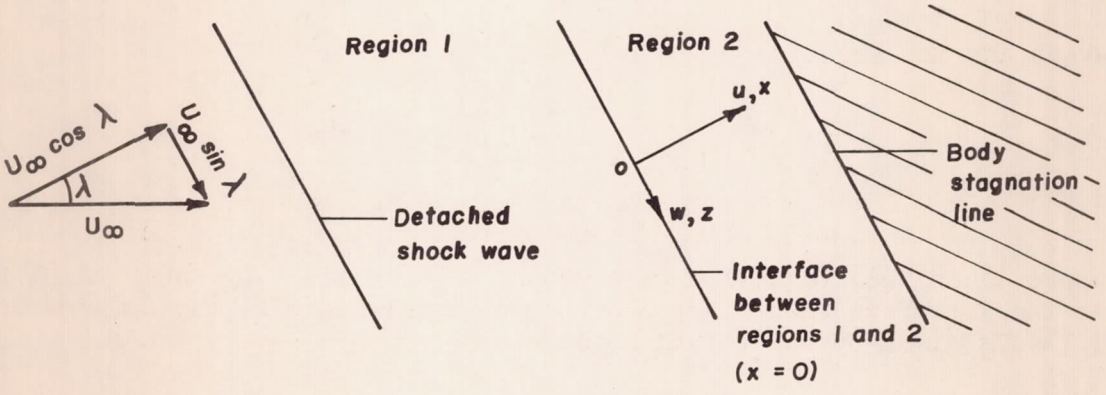

Region 1— Incompressible, nonviscous flow

Region 2— Compressible, viscous flow

Sketch (c)

The y momentum equation in region 1, differentiated with respect to y, takes the same form as equation (10) on the stagnation streamline. Thus the velocity u is again given by the solution

$$u = -\frac{1}{C}\sqrt{-\frac{1}{\rho}\frac{\partial^2 p}{\partial y^2}}\sinh Cx \tag{41}$$

The z momentum equation for the stagnation streamline in region 1 becomes, on dropping the negligible terms from equation (3),

$$u\frac{\partial w}{\partial x} = 0 \tag{42}$$

which has the solution

$$w^2 = \gamma_\infty R T_\infty M_\infty{}^2 \sin^2\lambda \tag{43}$$

since the transverse component of velocity is unchanged on passing through the shock wave.

The energy equation for the stagnation streamline in region 1 reduces to a form similar to equation (22)

$$u\frac{\partial u}{\partial x} + w\frac{\partial w}{\partial x} + C_p\frac{\partial T}{\partial x} = 0 \tag{44}$$

which has the solution

$$\int_T^{T_t} C_p dT = \frac{u^2 + \gamma_\infty R T_\infty M_\infty{}^2 \sin^2\lambda}{2} \tag{45}$$

where again the stagnation temperature T_t is given by equation (24). At the interface where the velocity u is negligible, the temperature $T_o(\lambda)$ is given by the solution to

$$\int_{T_o(\lambda)}^{T_t} C_p dT = \frac{\gamma_\infty R T_\infty M_\infty{}^2 \sin^2\lambda}{2} \tag{46}$$

which, for a constant heat capacity, C_p, is

$$\frac{T_o(\lambda)}{T_\infty} = \left(\frac{\gamma_\infty R}{2C_p}\right) M_\infty{}^2 \cos^2\lambda \tag{47}$$

The differentiated y momentum equation for region 2 takes on the same form on the stagnation streamline as equation (16). Hence, the solution is

$$\mu \frac{\partial u}{\partial x} = - \frac{\partial^2 p}{\partial y^2} \frac{x^2}{2} - \mu_o(\lambda) \sqrt{- \frac{1}{\rho} \frac{\partial^2 p}{\partial y^2}} \tag{48}$$

and the body stagnation point coordinate is

$$[x_b(\lambda)]^2 = \frac{2\mu_o(\lambda)}{\sqrt{- \rho \frac{\partial^2 p}{\partial y^2}}} \tag{49}$$

Now, however, the second derivative of pressure is a function of the angle of yaw (see Appendix B),

$$\left(\rho \frac{\partial^2 p}{\partial y^2}\right)_s = - \frac{6\rho_\infty{}^2 U_\infty{}^2 \cos^2\lambda}{(\gamma_s - 1) R_s{}^2} \tag{50}$$

so the stagnation-point coordinate is given by

$$\frac{x_b(\lambda)}{R_b} = \left(\frac{\gamma_s - 1}{6}\right)^{1/4} \left(\frac{\mu_o(\lambda)}{\mu_\infty} \frac{R_s}{R_b}\right)^{1/2} \frac{2}{Re_\infty{}^{1/2} \cos^{1/2}\lambda} \tag{51}$$

In region 2, the solutions to the z momentum equation and the energy equation are considered simultaneously. The z momentum equation simplifies (to the order of this analysis), in the region of the stagnation streamline, to

$$\frac{\partial}{\partial x}\left(\mu \frac{\partial w}{\partial x}\right) + \frac{\partial}{\partial y}\left(\mu \frac{\partial w}{\partial y}\right) = 0 \tag{52}$$

Similarly, the energy equation near the stagnation streamline in region 2 may be written (note that $\partial w/\partial y$ is zero by symmetry)

$$\frac{\partial^2 \eta}{\partial x^2} + \frac{\partial^2 \eta}{\partial y^2} + \mu \left(\frac{\partial w}{\partial x}\right)^2 = 0 \tag{53}$$

In order to facilitate the solution of equation (52), it is helpful to observe that the yawed boundary layer, identified with the w component of velocity, resembles the boundary layer on a flat plate. It might be anticipated then that, just as in the case of the flat plate, the variation of w with x is relatively insensitive to variations of μ with x. In this event equation (52) has the approximate form

$$\frac{\partial^2 w}{\partial x^2} + \frac{\partial^2 w}{\partial y^2} = 0 \tag{54}$$

The solution is taken in polar coordinates in order to conveniently fit the boundary condition that w is identically zero at the body surface. Then following the same arguments used in deriving equations (29) and (30), one obtains on the stagnation streamline

$$w = B \ln \frac{\bar{r}}{R_b} + \sum_{n=1}^{\infty} C_n \bar{r}^n \left[1 - \left(\frac{R_b}{\bar{r}}\right)^{2n}\right] = I\left(\epsilon - \frac{\epsilon^2}{2}\right) + O(\epsilon^3) \tag{55}$$

where again $\epsilon = (\bar{r}/R_b) - 1 << 1$. If second order and higher terms in ϵ are neglected, the z component of velocity on the stagnation streamline becomes, in terms of x/x_b,

$$w = w_o \left(1 - \frac{x}{x_b}\right) \tag{56}$$

whence

$$\frac{\partial w}{\partial x} = - \frac{w_o}{x_b} \tag{57}$$

If this result is substituted for the last term in equation (53), the energy equation becomes

$$\frac{\partial^2\eta}{\partial x^2} + \frac{\partial^2\eta}{\partial y^2} + \mu\left(\frac{w_o}{x_b}\right)^2 = 0 \tag{58}$$

A solution for equation (58) which satisfies symmetry conditions on the stagnation streamline and also the boundary conditions that η and μ are constant along the surface of the body is

$$\eta(\lambda) = \eta_b + B \ln\frac{\bar{r}}{R_b} + \sum_{n=1}^{\infty} C_n \bar{r}^n\left[1 - \left(\frac{R_b}{\bar{r}}\right)^{2n}\right]\cos n\theta - \frac{\bar{\mu}}{4}\left(\frac{w_o}{x_b}\right)^2(\bar{r}^2 - R_b^2) \tag{59}$$

where $\bar{\mu}$ is a mean value of μ in the stagnation region. If equation (59) is expanded in terms of ϵ, η takes the following form on the stagnation streamline

$$\eta(\lambda) = \eta_b + J\left(\epsilon - \frac{\epsilon^2}{2}\right) - \frac{\bar{\mu}w_o^2}{2\epsilon_o^2}\left(\epsilon + \frac{\epsilon^2}{2}\right) + O(\epsilon^3) \tag{60}$$

The constant J is evaluated by letting η be η_o when ϵ is $\epsilon_o = x_b/R_b$ and is given by the relation

$$J = \frac{\eta_o - \eta_b}{\epsilon_o}\left(1 + \frac{\epsilon_o}{2}\right) + \frac{\bar{\mu}w_o^2}{2\epsilon_o^2}(1 + \epsilon_o) + \cdots \tag{61}$$

The rate of heat transfer per unit area to the stagnation region of the body at angle of yaw λ is, from equation (60),

$$-\left.\frac{\partial\eta(\lambda)}{\partial x}\right|_b = \frac{1}{R_b}\left.\frac{\partial\eta(\lambda)}{\partial\epsilon}\right|_b = \frac{1}{R_b}\left(J - \frac{\bar{\mu}w_o^2}{2\epsilon_o^2}\right) \tag{62}$$

Substituting equations (26) and (61) into this expression and neglecting terms of the order ϵ_o compared to 1, one obtains

$$-\eta_b'(\lambda) = \frac{1}{x_b(\lambda)}\left(\int_{T_b}^{T_o(\lambda)} k\,dT + \frac{\bar{\mu}w_o^2}{2}\right) \tag{63}$$

Multiplying by $\frac{2R_b}{k_o(T_o - T_b)}$ and substituting from equation (51) yields

$$-\frac{2\eta_b'(\lambda)R_b}{k_o(T_o - T_b)} = \left(\frac{6}{\gamma_s - 1}\right)^{1/4}\left(\frac{\mu_\infty}{\mu_o(\lambda)}\frac{R_b}{R_s}\right)^{1/2}\frac{Re_\infty^{1/2}\cos^{1/2}\lambda}{k_o(T_o - T_b)}$$

$$\left(\int_{T_b}^{T_o(\lambda)} k\,dT + \frac{\bar{\mu}w_o^2}{2}\right) \tag{64}$$

For a constant heat capacity it follows from equations (23), (43), and (47) that

$$\left.\begin{aligned}\frac{T_o(\lambda)}{T_o} &= \cos^2\lambda \\ \frac{w_o^2}{T_o} &= 2C_p\sin^2\lambda\end{aligned}\right\} \tag{65}$$

If, in addition, the thermal conductivity is proportional to the nth power of temperature, then

$$\frac{1}{k_o(T_o - T_b)}\int_{T_b}^{T_o(\lambda)} k\,dT = \frac{\cos^{2n+2}\lambda}{(n+1)(1 - T_b/T_o)}\left[1 - \left(\frac{T_b}{T_o\cos^2\lambda}\right)^{n+1}\right] \tag{66}$$

and

$$\frac{\bar{\mu}w_o^2}{2k_o(T_o - T_b)} = \left(\frac{\bar{\mu}}{\mu_o}\right)\frac{Pr\sin^2\lambda}{1 - T_b/T_o} = \frac{\bar{\mu}}{\mu_o(\lambda)}\frac{Pr\cos^{2n}\lambda\sin^2\lambda}{1 - T_b/T_o} \tag{67}$$

Thus equation (64) becomes

$$-\frac{2\eta_b' R_b}{k_o(T_o - T_b)} = \frac{1}{n+1}\left(\frac{6}{\gamma_s - 1}\right)^{1/4}\left(\frac{R_b}{R_s}\right)^{1/2}\left(\frac{2C_p}{\gamma_\infty R}\right)^{n/2}\frac{Re_\infty^{1/2}\cos^{n+1/2}\lambda}{M_\infty^{n}(1 - T_b/T_o)}$$

$$\left\{\cos^2\lambda\left[1 - \left(\frac{T_b}{T_o\cos^2\lambda}\right)^{n+1}\right] + (n+1)\Pr\frac{\bar{\mu}}{\mu_o(\lambda)}\sin^2\lambda\right\} \tag{68}$$

The ratio of equation (68) to equation (39) is the ratio of the rate of heat transfer to the stagnation region of a yawed body to the rate of heat transfer to the stagnation region of the same body at zero yaw. This ratio is

$$\frac{\eta_b'(\lambda)}{\eta_b'(o)} = \frac{\cos^{n+1/2}\lambda}{1 - (T_b/T_o)^{n+1}}\left\{\cos^2\lambda\left[1 - \left(\frac{T_b}{T_o\cos^2\lambda}\right)^{n+1}\right] + (n+1)\Pr\frac{\bar{\mu}}{\mu_o(\lambda)}\sin^2\lambda\right\} \tag{69}$$

An analogous expression can be obtained for the ratio of Nusselt numbers, thus,

$$\frac{Nu(\lambda)}{Nu(o)} = \frac{\eta_b'(\lambda)}{\eta_b'(o)}\left(\frac{T_o}{T_r}\right)^{n}\frac{T_o - T_b}{T_r - T_b} \tag{70}$$

where from equation (63) the recovery temperature, T_r, is the solution to

$$\int_{T_r}^{T_o(\lambda)} k\, dT = -\frac{\bar{\mu}w_o^2}{2} \tag{71}$$

However, it should be noted that the assumptions used in the analysis tend to be violated when the body temperature approaches recovery conditions. Therefore it should not be expected that equation (71) will yield accurate values for recovery temperature.

There remains, of course, the problem of determining $\bar{\mu}$. It is sufficient for the purposes of this report to take $\bar{\mu}$ as simply the arithmetic average between $\mu_o(\lambda)$ and μ_b, that is, $\bar{\mu} = [\mu_o(\lambda) + \mu_b]/2$.[4] In this event equation (69) can be written

$$\frac{\eta_b'(\lambda)}{\eta_b'(o)} = \frac{\cos^{n+1/2}\lambda}{1 - (T_b/T_o)^{n+1}}\left\{\cos^2\lambda\left[1 - \left(\frac{T_b}{T_o\cos^2\lambda}\right)^{n+1}\right] + \frac{n+1}{2}\,Pr\left[1 + \left(\frac{T_b}{T_o\cos^2\lambda}\right)^{n}\right]\sin^2\lambda\right\} \tag{72}$$

which in the case of a relatively cool surface (i.e., $T_b/T_o\cos^2\lambda << 1$) becomes

$$\frac{\eta_b'(\lambda)}{\eta_b'(o)} = \cos^{n+1/2}\lambda\left(\cos^2\lambda + \frac{n+1}{2}\,Pr\,\sin^2\lambda\right) \tag{73}$$

These considerations complete the theoretical analysis. Attention is turned next to the experimental investigation.

EXPERIMENT

Test Apparatus

In order to investigate hypersonic heat-transfer phenomena, it was undertaken to develop an apparatus capable of producing a hot hypersonic air stream. In addition to the air stream being hot (i.e., characterized by stagnation temperatures of the order of thousands of degrees Rankine),

---

[4]Actually this procedure might better be considered the first step in an iteration method where $\bar{\mu}$ is recalculated on the basis of the preceding calculation of T as a function of x. This refinement is not considered warranted here where only the gross effects of yaw for angles of yaw well less than 90° are of principal interest. As the angle of yaw approaches 90°, the analysis as a whole tends to break down due to the violation of the several assumptions predicated on the flow being hypersonic normal to the axis of the cylinder.

it was required that the stream be of sufficient duration to facilitate measurements of heat transfer. The apparatus which finally evolved is termed a hypersonic gun tunnel simply because it combines a gun with a wind tunnel. Inasmuch as this gun tunnel has not been described in generally available literature, a brief description of its operation, calibration, and performance will be given here.

A schematic diagram of the equipment is shown in figure 1. A smooth-bore gun is used essentially as a one-stroke pump to create a reservoir of high-pressure, high-temperature air. A charge of fast burning powder is burned at the breech to accelerate the light-weight piston to a high velocity in the barrel. The accelerating piston produces strong shock waves which reflect a number of times from the blanked end of the barrel and the piston. These shock waves compress the air in the gun barrel in a highly nonisentropic manner, transforming much of the energy available in the powder charge to the form of heat in the air. Accordingly, a reservoir of very high-temperature air should be created.[5] As soon as equilibrium pressures have been reached in the reservoir, the valve closing the entrance to the nozzle is opened and the high-temperature, high-pressure air expands through the nozzle into the test section where models are located.

Figure 2 is a photograph of the present model of the hypersonic gun tunnel. This unit consists of a 20-mm smooth-bore barrel 5 feet long with a breech chambered for the standard 60/20 cartridge. The barrel is initially charged with dry air at 10 atmospheres pressure and room temperature.[6] A 20-mm diameter piston constructed of nylon and weighing 3-3/4 grams is used, and the cartridge is loaded with 27 grams of IMR No. 4227 rifle powder. The nozzle valve is released 80 milliseconds after the powder charge is ignited. In this time the reservoir conditions, as indicated by pressure measurements, have approached steady values. The flow exhausts through the nozzle into a vacuum tank. This tank, seen in figure 2, has a volume of 10 cubic feet and is pumped down to a pressure less than 0.0007 atmosphere before each test. In this manner sufficient compression ratio (up to 45×10^4) is provided across the nozzle to maintain hypersonic flow in the test section during the course of the run.

The nozzle through which the flow expands is fabricated of stainless steel and has a simple conical contour of 9° total angle and a 1-inch

---

[5] In Appendix E an estimate is made of the final temperatures that may be obtained from this nonisentropic compression. It is indicated that for a compression ratio of about 32, the ratio of final to initial temperature would be between 4 and 7. The corresponding isentropic compression process would yield a final to initial temperature ratio of only about 2.

[6] Higher final air temperatures should, of course, be obtained if the initial air temperatures are increased. This possibility is presently being investigated.

exit diameter (see fig. 3). While the flow is thus expanding conically, the rate of expansion is slow in the region of the models and for most practical purposes the flow may be considered parallel. The throat of the nozzle is a cylindrical section 0.020-inch in diameter and 0.050-inch long. This section is machined as a separate insert and can be replaced when the nozzle throat becomes seriously eroded by the heated air. Because of the length of the throat section, several runs can usually be made with one insert before erosion becomes serious in the sense that it increases the effective sonic throat diameter.

Calibration of Flow

Properties of the hypersonic stream produced by the gun tunnel were obtained from the following four measurements: reservoir pressure, pitot pressure, static pressure, and stream velocity. The reservoir pressure was measured with the gage shown in figure 4(a). The piston of the gage was housed in an insert which connected to an orifice leading to the reservoir section of the barrel (figs. 1 and 2). The O-ring seal near the bottom of the piston prevented leakage from the reservoir to the atmosphere, and the entire unit was retained by a yoke which was bolted to the side of the reservoir. The piston transmitted the pressure force from the reservoir to strain-gage elements which were electrically connected to a conventional bridge circuit, amplifier, and recording oscilloscope. The time required for the reservoir pressure to reach equilibrium was deduced from measurements made with a low-sensitivity gage element. A typical record of the initial pressure pulses is shown in figure 5(a), and it can be seen that these pulses are damped in well less than 0.06 second. The measured peak values of the first pulse or two are probably lower than the actual pressure maxima because of the inertia of the gage.[7]

The reservoir pressures used for calibration were measured with a high-sensitivity-gage element which was mechanically stopped at 400 atmospheres so that the peak pressure would not damage the gage. The average pressure for all runs is shown in figure 5(b) together with the standard deviation from the average. This deviation was within ±10 percent. The timing pulse shown in the figure corresponds to the signal superimposed on the oscilloscope record when the nozzle valve was opened. This pulse was taken as the zero time reference for the beginning of flow through the nozzle.

The pitot pressure was measured with a conventional, strut-mounted probe constructed from a 0.050-inch O.D. hypodermic needle (fig. 4(b)) with an outer to inner diameter ratio (O.D./I.D.) of 1.47. The probe led

[7]It may be of interest that the frequency of these measured pulses is nearly identical to that predicted by the method of characteristics.

to a variable-capacitance diaphragm-type pressure cell (fig. 4(b)) connected to a bridge circuit, amplifier, and a recording oscilloscope. The response time of this system appeared to be instantaneous for practical purposes. The average value of the ratio of the pitot pressure (measured on the nozzle center line) to reservoir pressure is shown in figure 5(c). This ratio is approximately constant at 6.6×10^{-4} during the first 0.3 second but then, for some unexplained reason, jumps to a higher value and holds approximately constant until about 0.6 second.[8] For the first 0.3 second, standard deviation limits shown in figure 5(c) are within 4 percent of the average.

The static pressure was also measured with a conventional type probe consisting of a 13° included angle cone-cylinder combination of 0.050-inch O.D. mounted in the same manner as the pitot probe. The pressure orifices were located at the test station and, to determine if the measured values of static pressure were grossly influenced by Reynolds number effects or feedback, a series of probes were tested. These probes had forebodies and afterbodies that ranged from 30 to 60 diameters in length as measured from the pressure orifices to the tip of a probe and to the leading edge of the strut, respectively (fig. 4(c)). Each probe was connected to a capacitance pressure gage which differed in only one respect from that used for pitot pressure measurements. This difference was that a thinner diaphragm element was used in order to obtain the necessary instrument sensitivity at the lower static pressures. The pressures measured on the nozzle center line with the several probes were essentially in agreement, and the value of measured static to reservoir pressure for all runs is shown in figure 5(d). The standard deviation limits for the first 0.3 second are within 8 percent of the average.

Now it seems reasonable to expect that the stream static pressure actually varies like the pitot pressure during this interval of time; that is to say, changes in p/H with time (fig. 5(d)) are due primarily to the finite response time of the static pressure measuring system. With this thought in mind the measured data on p/H have been reduced in the manner described in Appendix F. The corrected value of p/H is found to be 5.32×10^{-6} for the first 0.3 second of run. The corresponding value of p/p_t during this interval is 8.06×10^{-3}.

Pitot and static pressures were also measured 1/8-inch off the nozzle center line, and they were found to agree with the center-line measurements to within the standard deviation.

---

[8] The flow does not actually choke to subsonic speeds until about 1.0 second, but after 0.6 second it is rather erratic. Accordingly, the flow was calibrated only over the interval from 0 to 0.6 second. It was found that the jump in pitot pressure occurring between 0.3 and 0.4 second is accompanied by unpredictable changes in static pressure, in shock-wave profiles about models, and in heat-transfer measurements.

The stream velocity was obtained by determining the rate at which a disturbance passes through the test section. This disturbance was produced by the spark discharge of a 0.5 mfd capacitance at 10 kilovolts across electrodes mounted in the stream ahead of the test region (see fig. 4(d)). The position of the disturbance in the test region was recorded photographically with a schlieren apparatus using a spark discharge light source. The velocity of the stream was then taken as the distance between the tips of the spark electrodes and the center of the disturbance divided by the time interval between the disturbance spark discharge and the schlieren exposure.[9] Some typical schlieren photographs of different disturbances are shown in figure 6(a). (At the bottom of the test region can be seen a blunt test probe and its associated shock-wave system.) Measurements of velocity were made for separate runs over the range of flow time from 0.03 to 0.60 second. The flow time was again measured from the opening of the nozzle valve. At each flow time, a series of runs were made in which the time interval between the disturbance discharge and the schlieren exposure was varied. The data, shown plotted in figure 6(b), appear to be relatively independent of this time interval, and it is therefore concluded that any consistent error existing in the velocity measurements is small.

The reservoir pressure was not used directly to determine stream properties, since it was considered unjustifiable to assume that the expansion of air from reservoir to test region satisfied the usual isentropic relations. However, the reservoir pressure was used to nondimensionalize the measured static and pitot pressures, inasmuch as the ratios p/H and p_t/H were more consistent from run to run than the absolute pressures. Pertinent stream properties were then determined in the following manner. At hypersonic Mach numbers, the ratio of pitot pressure p_t to dynamic pressure q_∞ is approximately independent of Mach number, namely,

$$\frac{\rho_t}{2q_\infty} = \frac{p_t}{\rho_\infty U_\infty^2} = \Gamma(\gamma) = \left(\frac{1}{\gamma}\right)^{\frac{\gamma}{\gamma-1}} \left(\frac{\gamma+1}{2}\right)^{\frac{\gamma+1}{\gamma-1}} \tag{74}$$

The function $\Gamma(\gamma)$ is very nearly constant, varying only from 0.920 to 0.977 as γ varies from 1.4 to 1.1. Then, the unknown stream parameters are, in terms of the measured properties

$$\left.\begin{aligned} &\text{density, } \rho_\infty = p_t/\Gamma U_\infty^2 \\ &\text{static temperature, } T_\infty = p_\infty/\rho_\infty R = (\Gamma U_\infty^2/R)\, p_\infty/p_t \\ &\text{Mach number, } M_\infty = \sqrt{U_\infty^2/\gamma_\infty R T_\infty} = \sqrt{(p_t/p_\infty)/\gamma_\infty \Gamma} \end{aligned}\right\} \tag{75}$$

[9]The electrodes were of slender (15° wedge 0.075 inch thick at root) cross section in the streamwise direction, so that while they might alter stream Mach number, they were unlikely to appreciably influence stream velocity at the hypersonic speeds of these tests.

and the stagnation temperature T_t is the solution to

$$\int_T^{T_t} C_p dT = \frac{U_\infty^2}{2} \tag{76}$$

The measured velocity of the stream is nominally 5000 ft/sec.[10] Then, if ideal gas values are used for heat capacity in equation (76), the stagnation temperature is 2200° R. If vibrational energy modes are fully excited in any part of the flow, the correction for this caloric imperfection might decrease the stagnation temperature to 2100° R (see refs. 9 and 10). This correction is within the deviation in velocity data, however, and therefore was not applied.

The ratio of static to pitot pressure, 8.06×10^{-3}, yields a Mach number of 9.8 (eq. (75)) and the initial values of the pitot and static pressure are 0.224 and 0.0018 atmosphere, respectively. These pressures, and therefore the density also, fall off approximately exponentially during the flow. Accordingly, the nominal free-stream Reynolds number also decreases with time and is given approximately by the relation, $Re = 1.26\ e^{-t/0.6}$ million per foot.

The stream properties given above are all reproducible within 10 percent. It will be noted that the stream velocity appears somewhat lower than the nominal value at the beginning of the flow (see fig. 6(b)). This result may be due to the initial cooling effect of the sonic throat region and the reservoir. In any case, however, this decrease in velocity is within the standard deviation of the data, and the nominal value of velocity will accordingly be taken as 5000 ft/sec for the entire interval of flow.

In addition to the above calibration, the purity of the air stream was tested by analyzing gas samples with a mass spectrometer and samples of condensable phase impurities by X-ray diffraction and emission spectrograph methods. The gas samples were collected with a pitot tube leading to an evacuated glass flask. At a predetermined time of flow, the copper tubing leading to the flask was sealed with a hydraulic pinch. The condensable phase impurities were simply collected by impact on a spectrographic grade copper rod and time scale effects were differentiated by using a movable rod within a shield.

It was found that the gas samples were essentially normal air except for about 1-percent carbon dioxide and a trace of nitrous oxide. As expected, the percentage of these impurities increased as the sampling

[10] Velocities up to about 8000 ft/sec have been obtained using larger powder charges. This result implies stagnation temperatures in excess of 5000° R. Damage to the gun barrel was, however, excessive to the point of being intolerable under these circumstances.

time interval was lengthened. The condensable phase impurity was found to be iron oxide, undoubtedly originating from observed areas of erosion in the reservoir and the nozzle throat. Samples taken at the beginning of flow showed very light film deposits of impurities, and for this reason it is felt that the initial heat-transfer rates measured at the beginning of flow should most nearly represent the correct values for normal air.[11] Therefore, only these initial data are interpreted in the following portions of this paper. This procedure also serves essentially to eliminate the problem of evaluating heat-loss corrections for the heat-transfer models since these corrections must vanish at zero time when thermal gradients along a model are zero.

Heat-Transfer Models and Reduction of Data

The models used in the heat-transfer experiments were tested at the same station at which the pitot and static pressure data were taken. These models were butt-welded iron-constantan thermocouple cylinders (fig. 7(a)) transverse to the flow at various angles of yaw. Wires of 0.003-, 0.010-, 0.012-, 0.020-, and 0.040-inch diameter were tested at zero yaw. The 0.003-inch-diameter wire was tested at 22.5°, 45°, and 70° angle of yaw and the 0.020-inch diameter wire was tested at 45° yaw (shown installed in the test region, fig. 7(b)).[12] The thermocouple junctions were examined microscopically and were rejected if the weld showed visible imperfection.

The diffusivity of the thermocouple material was sufficiently large to permit the assumption that temperature gradients across the thermocouple junction were negligible (i.e., the time of diffusion to within 95 percent of constant temperature is very much less than the time constant of response of the thermocouple to heat transfer from the air stream). Thus the average rate of heat transfer per unit area to the models was proportional to the rate of change of temperature indicated by the thermocouple junction. Under these conditions the average heat-transfer rate satisfies the relation

$$-\bar{\eta}_b' = \frac{R_b C_b \rho_b}{2} \frac{dT_b}{dt} \tag{77}$$

[11]The possibility of these impurities causing errors in the heat-transfer data is considered further in Appendix F.

[12]The ratio of length to diameter of all test cylinders was 25 or greater. In the case of the yawed cylinders this ratio was always in excess of 50. Accordingly, it is felt that end effects on measured heat-transfer rates are negligible, with the possible exception of the data for 70° yaw.

where T_b is the temperature of the thermocouple with radius R_b, specific heat C_b, and density ρ_b (note $C_b\rho_b$ is essentially the same for iron and constantan). It is convenient in the analysis of data for the cylinders at zero yaw to employ an average heat-transfer coefficient $\bar{h}$ defined by the equation

$$\bar{h} = \frac{-\bar{\eta}_b'}{T_t - T_b} \tag{78}$$

It follows that the average Nusselt number, based on stagnation temperature conditions and a characteristic length equal to the diameter of a cylinder, is given by the expression

$$\overline{Nu} = \frac{2\bar{h}R_b}{k_t} = \frac{R_b^2 C_b \rho_b}{k_t(T_t - T_b)} \frac{dT_b}{dt} \tag{79}$$

Figure 8(a) shows the output from the 0.003-inch-diameter transverse thermocouple for a typical zero-yaw run. The rate of temperature rise drops below expected values after about 0.05 second. At about 0.3 second the record indicates some perturbation in the flow as did the static and pitot pressure measurements, and observed shock-wave profiles. The initial temperature rise, which is of principal interest here, repeated to within ±10 percent from run to run. In order to measure this initial rise more accurately, the oscilloscope sweep speeds were adjusted to give about 45° slope of the temperature-time curve. A typical temperature-rise curve on the expanded time scale is shown in figure 8(b).

RESULTS AND DISCUSSION

The theory of this report treats, of course, only the heat transfer to the stagnation region of a body in hypersonic flow. Nevertheless, for a relatively blunt body, such as a transverse cylinder, it seems reasonable to expect that in hypersonic flow, just as in lower speed flow, the average rate of heat transfer will vary in proportion to the stagnation-region heat-transfer rate. With this thought in mind, it is noted that according to equation (39) for a cylindrical stagnation region ($\lambda = 0$, $n = 1/2$, $T_b/T_o << 1$)

$$Nu \sim \sqrt{\left(\frac{Re_\infty}{M_\infty}\right)\left(\frac{R_b}{R_s}\right)} \tag{80}$$

If R_b/R_s is considered constant (presumably at some value near 1), then it is easily demonstrated that

$$Nu \sim \sqrt{\frac{Re_\infty}{M_\infty}} \sim \sqrt{Re_s} \tag{81}$$

neglecting small differences between μ_o and μ_s. This is essentially the result deduced experimentally by Kovaznay (ref. 11) and by others for the average Nusselt numbers of cylinders transverse to subsonic and supersonic flows. The experimental data obtained in the hypersonic gun tunnel should provide some indication of whether or not the result holds in the same sense for hypersonic flows. These data for transverse cylinders are presented in figure 9,[13] along with the predictions of equation (81) (replacing Nu with $\overline{Nu}$) and with data obtained from hot-wire type experiments by Kovaznay (ref. 11), Stine (ref. 12), and Stalder, Goodwin and Creager (ref. 13). Specifically, there are shown (after the method of Stine) the average Nusselt numbers as a function of $M_\infty/Re_\infty Pr$. The agreement between the data obtained from the hypersonic gun tunnel and those obtained by the hot-wire method is surprisingly good considering the wide difference in test conditions[14] (e.g., as contrasted to the gun-tunnel data, the data of reference 12 are for Mach numbers less than 1.4 and stagnation temperatures less than 590° R). Note, too, that the scatter of the data from the gun tunnel is by and large of no greater order of magnitude than that of the data in references 11, 12, and 13. Finally, it is observed that equation (81) is quite as consistent with experiment at hypersonic speeds as it is at lower speeds. Evidently, then, average rates of heat transfer to transverse cylinders in hypersonic flow do tend to vary in proportion to the stagnation-region heat-transfer rates.

It is appropriate to inquire now about the effect of yaw on the rate of heat transfer to a cylinder in hypersonic flow. In this regard it is of interest to see first what theory predicts for the effect of yaw on heat transfer to a cylindrical stagnation region. Two cases will be treated, namely, $T_b/T_o = 0$ and $T_b/T_o = 0.24$, the value corresponding to test conditions in the hypersonic gun tunnel. If Prandtl number is taken equal to 3/4, and the temperature exponent for the thermal conductivity

---

[13]Note that while the test Reynolds numbers are low, they are, according to estimate, within the range of continuum laminar flow.

[14]While the stagnation temperatures of the hypersonic gun tunnel were far greater than those of the other tests, it should be noted that they were well below temperatures at which dissociation might be expected to occur and, hence, possibly influence heat transfer.

and viscosity functions is taken as 1/2,[15] then according to equation (72) the stagnation-region heat-transfer rate is influenced by yaw in the manner shown on figure 10. For the case of $T_b/T_o = 0$, it is indicated that yaw should reduce the rate of heat transfer almost in proportion to $\cos^2\lambda$ (note this is the same reduction factor as for impact pressures). For the case of $T_b/T_o = 0.24$ the predicted reduction in rate of heat transfer is somewhat less, although still very sizable. How well this prediction agrees with measurements of average heat-transfer rates to yawed cylinders in the hypersonic gun tunnel is shown in figure 11. The average rates are observed to decrease with increasing yaw in much the manner predicted by the stagnation-region theory. For example, at 70° yaw, theory and experiment show about a 60-percent reduction in heat-transfer rate.

The stagnation-region theory and hypersonic gun-tunnel experiments have, then, provided useful information on the problem of heat transfer to cylinders in hypersonic flow. However, all of the considerations, both theoretical and experimental, up to this point have been for the case where the gas does not dissociate and therefore the gas properties vary with temperature in a somewhat ideal manner. At the very high temperatures encountered in hypersonic flight (namely, at temperatures in excess of about 5000° R) gas molecules may dissociate into atoms. It is natural then to inquire how dissociation might alter our previous conclusions. Accordingly, the effects of equilibrium dissociation on the rate of heat transfer to a cylindrical stagnation region at zero yaw have been examined theoretically in Appendix G. The calculated heat-transfer rates are increased by dissociation at Mach numbers greater than 10 (see fig. 12). It is suggested, then, that equilibrium dissociation (should it occur) may alter our previous conclusions regarding the effect of yawing a cylinder to the extent that somewhat greater reductions in heat-transfer rates will be achieved. This possibility derives from the fact that the high temperatures which bring about dissociation tend to be decreased by yaw.[16]

CONCLUDING REMARKS

It has been argued theoretically and demonstrated experimentally that yaw can have the effect of substantially reducing the rate of heat transfer

---

[15]The 1/2 power law is, at the very high temperatures encountered in hypersonic flight, a rather good approximation according to Sutherland's equation (C_p = const), although actually the results of theory are relatively insensitive to n (except at very large yaw) over the range $1/2 < n < 3/4$.

[16]It is perhaps worthy of note, too, that by the same token radiation heat transfer from the high temperature disturbed air to the body surface should be alleviated by yaw.

to a circular cylinder in hypersonic flow. Experiments on small cylinders in a hypersonic air stream of Mach number 9.8 and stagnation temperature 2200° R tended to verify this prediction, indicating that the rate of heat transfer was reduced to about 40 percent of its zero-yaw value when the angle of yaw was 70°. These results are interpreted to have the practical significance that sweep may markedly reduce the heat transfer per unit area to the blunt leading edge of a wing in hypersonic flight.

Ames Aeronautical Laboratory
National Advisory Committee for Aeronautics
Moffett Field, Calif., May 2, 1955

APPENDIX A

SIMPLIFICATION OF THE y MOMENTUM EQUATION IN REGION 2

The steady-state, two-dimensional y momentum equation (see eq. (2)), differentiated with respect to y, yields

$$\rho u \frac{\partial^2 v}{\partial x \partial y} + u \frac{\partial \rho}{\partial y} \frac{\partial v}{\partial x} + \rho \frac{\partial v}{\partial x} \frac{\partial u}{\partial y} + \rho v \frac{\partial^2 v}{\partial y^2} + v \frac{\partial \rho}{\partial y} \frac{\partial v}{\partial y} + \rho \left(\frac{\partial v}{\partial y} \right)^2$$

$$= - \frac{\partial^2 p}{\partial y^2} - \frac{2}{3} \frac{\partial^2}{\partial y^2} \left[\mu \left(\frac{\partial u}{\partial x} + \frac{\partial v}{\partial y} \right) \right] + 2 \frac{\partial^2}{\partial y^2} \left(\mu \frac{\partial v}{\partial y} \right) + \frac{\partial^2}{\partial y \partial x} \left[\mu \left(\frac{\partial u}{\partial y} + \frac{\partial v}{\partial x} \right) \right] \quad \text{(A1)}$$

Now on the stagnation streamline the velocity v is identically zero and therefore all x derivatives of v are zero. Also, all odd order y derivatives of functions like density ρ, viscosity μ, pressure p, and velocity u vanish since, by symmetry, these functions are even. In addition, it is assumed that near the stagnation streamline the velocity u is so small throughout region 2 that terms with this factor may be neglected. With this assumption an additional useful relation can be deduced from the continuity equation

$$\rho \frac{\partial u}{\partial x} + u \frac{\partial \rho}{\partial x} + \rho \frac{\partial v}{\partial y} + v \frac{\partial \rho}{\partial y} = 0 \quad \text{(A2)}$$

Eliminating the terms with factors u, v, or $\partial \rho / \partial y$ from equation (A2) there results, as for incompressible flow,

$$\frac{\partial u}{\partial x} + \frac{\partial v}{\partial y} = 0 \quad \text{(A3)}$$

Note that all derivatives of the sum $\partial u/\partial x + \partial v/\partial y$ are also zero in the regions where equation (A3) will hold.

Applying the above considerations simplifies equation (A1) to

$$\rho \left(\frac{\partial v}{\partial y} \right)^2 = - \frac{\partial^2 p}{\partial y^2} + 2 \frac{\partial^2}{\partial y^2} \left(\mu \frac{\partial v}{\partial y} \right) + \frac{\partial^2}{\partial y \partial x} \left[\mu \left(\frac{\partial u}{\partial y} + \frac{\partial v}{\partial x} \right) \right] \quad \text{(A4)}$$

Now it will be assumed, as is usual, that the viscous flow in the region of the stagnation point of a blunt body is similar to viscous flow at the stagnation point of a body with infinite radius of curvature insofar as the velocity derivatives are concerned (i.e., the principle effect of the body curvature is to determine the magnitude of the pressure derivatives). Accordingly, $\partial^3 v/\partial y^3$ and $\partial^2 u/\partial y^2$ will be supposed to vanish in the stagnation region. Then expansion of the second member of the right side of equation (A4) yields

$$2\left(\frac{\partial^2 \mu}{\partial y^2}\frac{\partial v}{\partial y} + 2\frac{\partial \mu}{\partial y}\frac{\partial^2 v}{\partial y^2} + \mu\frac{\partial^3 v}{\partial y^3}\right)$$

in which the only term retained is $2(\partial^2\mu/\partial y^2)(\partial v/\partial y)$. Similar expansion of the last member of equation (A4) gives

$$\frac{\partial^2 \mu}{\partial x \partial y}\left(\frac{\partial u}{\partial y} + \frac{\partial v}{\partial x}\right) + \frac{\partial \mu}{\partial y}\left(\frac{\partial^2 u}{\partial x \partial y} + \frac{\partial^2 v}{\partial x^2}\right) + \frac{\partial \mu}{\partial x}\left(\frac{\partial^2 u}{\partial y^2} + \frac{\partial^2 v}{\partial x \partial y}\right) + \mu\left(\frac{\partial^3 u}{\partial y^2 \partial x} + \frac{\partial^3 v}{\partial y \partial x^2}\right)$$

Note that from equation (A3), $\partial^3 u/\partial y^2 \partial x$ is equivalent to $-(\partial^3 v/\partial y^3)$ and will therefore be neglected. The terms retained in this equation, then, are $(\partial\mu/\partial x)(\partial^2 v/\partial x \partial y) + \mu(\partial^3 v/\partial y \partial x^2)$. These terms can be combined into $-\frac{\partial}{\partial x}\left(\mu\frac{\partial^2 u}{\partial x^2}\right)$. Equation (A4) thus is reduced to

$$\frac{\partial}{\partial x}\left(\mu\frac{\partial^2 u}{\partial x^2}\right) = -\frac{\partial^2 p}{\partial y^2} + 2\frac{\partial^2 \mu}{\partial y^2}\frac{\partial v}{\partial y} - \rho\left(\frac{\partial v}{\partial y}\right)^2 \tag{A5}$$

The derivative $\partial v/\partial y$ vanishes at the surface of the body, so that in the immediate region of the stagnation point, equation (A5) takes on the approximate from

$$\frac{\partial}{\partial x}\left(\mu\frac{\partial^2 u}{\partial x^2}\right) = -\frac{\partial^2 p}{\partial y^2} \tag{A6}$$

This expression will be taken to hold near the stagnation streamline throughout region 2.

APPENDIX B

BOUNDARY VELOCITIES AND PRESSURE DERIVATIVES

For hypersonic Mach numbers, the density ratio across an oblique shock wave is

$$\frac{\rho_s}{\rho_\infty} = \frac{\gamma_s + 1}{\gamma_s - 1} \tag{B1}$$

then the pressure just downstream of the shock is

$$p_s = \frac{2\rho_\infty U_\infty^2 \cos^2\sigma}{\gamma_s + 1} \tag{B2}$$

where σ is the acute angle between the shock wave and the normal to the free-stream velocity vector (see ref. 9). It can also be shown that the v component of velocity just downstream of the shock is

$$v_s = \frac{2}{\gamma_s + 1} U_\infty \sin\sigma \cos\sigma \tag{B3}$$

while the u component on the stagnation streamline is

$$u_s = \frac{\gamma_s - 1}{\gamma_s + 1} U_\infty \tag{B4}$$

In evaluating the derivatives, consider a shock wave with radius of curvature R_s. Let s be the distance along this profile measured from the stagnation streamline and $x(s)$ and $y(s)$ be the equations for the shock-wave coordinates. Then

$$\frac{dv}{ds} = \frac{\partial v}{\partial x}\frac{dx}{ds} + \frac{\partial v}{\partial y}\frac{dy}{ds} \tag{B5}$$

while

$$\frac{d^2p}{ds^2} = \frac{\partial^2 p}{\partial x^2}\left(\frac{dx}{ds}\right)^2 + 2\frac{\partial^2 p}{\partial x \partial y}\frac{dx}{ds}\frac{dy}{ds} + \frac{\partial^2 p}{\partial y^2}\left(\frac{dy}{ds}\right)^2 + \frac{\partial p}{\partial x}\frac{d^2x}{ds^2} + \frac{\partial p}{\partial y}\frac{d^2y}{ds^2} \tag{B6}$$

In terms of the radius of curvature R_s, the differential equations for x(s) and y(s) are

$$\left.\begin{aligned} dx &= R_s\left(1 - \cos\frac{ds}{R_s}\right) \\ dy &= R_s \sin\frac{ds}{R_s} \end{aligned}\right\} \tag{B7}$$

and at the stagnation streamline (ds = 0) the following conditions hold

$$\left.\begin{aligned} \frac{dy}{ds} &= 1 \\ \frac{dx}{ds} &= 0 \\ \frac{d^2y}{ds^2} &= 0 \\ \frac{d^2x}{ds^2} &= \frac{1}{R_s} \end{aligned}\right\} \tag{B8}$$

Then, at the stagnation streamline, equations (B5) and (B6) become

$$\left(\frac{\partial v}{\partial y}\right)_s = \frac{dv}{ds} \tag{B9}$$

and

$$\left(\frac{\partial^2 p}{\partial y^2}\right) = \frac{d^2p}{ds^2} - \frac{1}{R_s}\left(\frac{\partial p}{\partial x}\right)_s \tag{B10}$$

Now by continuity and equations (B3) and (B9)

$$\left(\frac{\partial u}{\partial x}\right)_s = -\left(\frac{\partial v}{\partial y}\right)_s = -\frac{2U_\infty}{(\gamma_s + 1)R_s} \tag{B11}$$

for two-dimensional flow. For axially symmetric flow the corresponding relation is

$$\left(\frac{\partial u}{\partial x}\right)_s = -2\left(\frac{\partial v}{\partial r}\right)_s = -\frac{4U_\infty}{(\gamma_s + 1)R_s} \tag{B12}$$

According to equation (B2) the first right-hand term of equation (B10) is

$$\frac{d^2p}{ds^2} = -\frac{4\rho_\infty U_\infty^2}{(\gamma_s + 1)R_s^2} \tag{B13}$$

while the next term, $-\frac{1}{R_s}\left(\frac{\partial p}{\partial x}\right)_s$, is evaluated using the x momentum equation (eq. (1)) which for the nonviscous incompressible flow region on the stagnation streamline reduces to

$$\frac{\partial p}{\partial x} = -\rho u \frac{\partial u}{\partial x} \tag{B14}$$

According to equations (B11) and (B12), equation (B14) becomes

$$\frac{\partial p}{\partial x} = \frac{2(\gamma_s - 1)}{(\gamma_s + 1)^2}\frac{\rho_s U_\infty^2}{R_s} \tag{B15}$$

and

$$\frac{\partial p}{\partial x} = \frac{4(\gamma_s - 1)}{(\gamma_s + 1)^2}\frac{\rho_s U_\infty^2}{R_s} \tag{B16}$$

for the two-dimensional and the axially symmetric flow cases, respectively. Then the corresponding second partial derivatives of pressure are

$$\frac{\partial^2 p}{\partial y^2} = -\frac{6(\gamma_s - 1)\rho_s U_\infty^2}{(\gamma_s + 1)^2 R_s^2} \tag{B17}$$

and

$$\frac{\partial^2 p}{\partial r^2} = - \frac{8(\gamma_s - 1)\rho_s U_\infty^2}{(\gamma_s + 1)^2 R_s^2} \tag{B18}$$

Note that γ_s can have values somewhat different than 1.4 if vibrational and dissociational energies are excited at the shock wave. The results of this appendix are consistent if γ_s is defined by equation (B1) from the ratio of densities across the shock wave. When additional energy modes are excited at the shock wave, this effective value of γ_s is not exactly the ratio of specific heats.

It can be seen that for the case of a yawed two-dimensional body, the same relations hold as for the body at zero yaw except that the velocity U_∞ is replaced by the normal component of velocity, $U_\infty \cos \lambda$. Thus the yawed two-dimensional body has a second derivative of pressure

$$\frac{\partial^2 p}{\partial y^2} = - \frac{6(\gamma_s - 1)\rho_s U_\infty^2 \cos^2 \lambda}{(\gamma_s + 1)^2 R_s^2} \tag{B19}$$

In the above relations the radius of curvature of the shock wave R_s is yet undetermined. In the limit of infinite free-stream Mach number, the ratio of shock wave to body curvature, R_s/R_b, might be expected to approach unity as an upper bound. On the other hand, a value of R_s/R_b consistent with incompressible boundary-layer solutions may be a reasonable lower bound. In this regard Howarth (ref. 7) reports that for two-dimensional flow

$$\frac{\partial v}{\partial y} = \frac{2u_s}{R_b} \tag{B20}$$

which, according to equations (B4) and (B11), corresponds to a ratio

$$\frac{R_s}{R_b} = \frac{1}{\gamma - 1} \tag{B21}$$

Sibulkin (ref. 14), using a similar analysis finds that

$$\frac{\partial v}{\partial y} = \frac{3U_s}{2R_b} \tag{B22}$$

for axially symmetric flow. This corresponds to the ratio

$$\frac{R_s}{R_b} = \frac{4}{3(\gamma - 1)} \tag{B23}$$

APPENDIX C

HEAT TRANSFER TO AN AXIALLY SYMMETRIC STAGNATION REGION

The methods used to calculate the rate of heat transfer to a cylindrical stagnation region can also be applied to the stagnation region of a spherical body. This analysis is parallel to that for the cylinder at zero yaw and thus the x axis is taken as the stagnation streamline and the origin of the coordinate system is placed at the interface between the assumed incompressible nonviscous region 1 and the viscous, low-velocity, compressible region 2. For the purpose of obtaining the solutions for velocity in regions 1 and 2 on the stagnation streamline, it is most convenient to consider the momentum and continuity equations in cylindrical coordinates. Because of axial symmetry, all properties are independent of the angular coordinate and, accordingly, the r direction momentum equation becomes

$$\rho\left(u\frac{\partial v}{\partial x}+v\frac{\partial v}{\partial r}\right)=-\frac{\partial p}{\partial r}-\frac{2}{3}\frac{\partial}{\partial r}\left[\mu\left(\frac{\partial u}{\partial x}+\frac{\partial v}{\partial r}+\frac{v}{r}\right)\right]+2\frac{\partial}{\partial r}\left(\mu\frac{\partial v}{\partial r}\right)+$$

$$2\frac{\mu}{r}\left(\frac{\partial v}{\partial r}-\frac{v}{r}\right)+\frac{\partial}{\partial x}\left[\mu\left(\frac{\partial u}{\partial r}+\frac{\partial v}{\partial x}\right)\right] \qquad (C1)$$

While the continuity equation is

$$\frac{\partial}{\partial x}(\rho u)+\frac{1}{r}\frac{\partial}{\partial r}(\rho r v)=0 \qquad (C2)$$

In region 1 where the viscous terms are considered identically zero, the r momentum equation (eq. (C1)) reduces to

$$\rho\left(u\frac{\partial v}{\partial x}+v\frac{\partial v}{\partial r}\right)=-\frac{\partial \rho}{\partial r} \qquad (C3)$$

Differentiating equation (C3) with respect to r and dropping terms with factors v and $\partial v/\partial x$, which vanish on the stagnation streamline, gives

$$\left(\frac{\partial v}{\partial r}\right)^2+u\frac{\partial^2 v}{\partial x\partial r}=-\frac{1}{\rho}\frac{\partial^2 p}{\partial r^2} \qquad (C4)$$

Now the continuity equation (eq. (C2)) expands to

$$\rho \frac{\partial u}{\partial x} + \frac{\rho v}{r} + \rho \frac{\partial v}{\partial r} = 0 \tag{C5}$$

however, on the axis of symmetry, neglecting terms higher than second order in r,

$$\frac{\partial v}{\partial r} = \frac{v}{r} \tag{C6}$$

Thus, for incompressible flow, the continuity equation on the stagnation streamline reduces to

$$\frac{\partial u}{\partial x} + 2 \frac{\partial v}{\partial r} = 0 \tag{C7}$$

Substituting equation (C7) into equation (C4) yields

$$\frac{1}{4}\left(\frac{\partial u}{\partial x}\right)^2 - \frac{u}{2} \frac{\partial^2 u}{\partial x^2} = - \frac{1}{\rho} \frac{\partial^2 p}{\partial r^2} \tag{C8}$$

which, upon differentiating with respect to x, and assuming $\frac{1}{\rho} \frac{\partial^2 p}{\partial r^2}$ = constant, becomes

$$u \frac{\partial^3 u}{\partial x^3} = 0 \tag{C9}$$

For nonzero values of the velocity u, this differential equation has as a solution

$$u = \frac{u_o''}{2} x^2 + u_o' x + u_o \tag{C10}$$

The value of velocity at the interface, u_o, is again considered very small. Thus, from equation (C8), the first derivative of velocity at the interface is, approximately,

$$u_o' = -\sqrt{\frac{4}{\rho}\frac{\partial^2 p}{\partial r^2}} \tag{C11}$$

As can be seen from the solution for velocity, equation (C10), the second derivative of velocity is constant. Therefore the second derivative of velocity may be evaluated from equation (C8) using conditions just behind the shock wave, thus,

$$u_o'' = \frac{u_s'^2}{2u_s} + \frac{2}{u_s\rho_s}\left(\frac{\partial^2 p}{\partial r^2}\right)_s \tag{C12}$$

Substituting for the values of velocity, velocity derivative, and second pressure derivative behind the shock wave (see Appendix B) yields

$$u_o'' = \frac{8(3 - 2\gamma_s)}{\gamma_s^2 - 1}\frac{U_\infty}{R_s^2} \tag{C13}$$

and

$$u_o' = -\frac{4\sqrt{2(\gamma_s - 1)}}{\gamma_s + 1}\frac{U_\infty}{R_s} \tag{C14}$$

Now in region 2, the viscous terms are retained in equation (C1). Following the procedure used in studying two-dimensional flow (see Appendix A), the r momentum equation, differentiated with respect to r, is simplified to

$$\frac{\partial}{\partial x}\left(\frac{\mu}{2}\frac{\partial^2 u}{\partial x^2}\right) = -\frac{\partial^2 p}{\partial r^2} \tag{C15}$$

which integrates to

$$\frac{\mu}{2}\frac{\partial^2 u}{\partial x^2} = -\frac{\partial^2 p}{\partial r^2}x + A \tag{C16}$$

and, as in the case of the two-dimensional flow,

$$\frac{\mu}{2}\frac{\partial u}{\partial x} = -\frac{\partial^2 p}{\partial r^2}\frac{x^2}{2} + Ax + B \tag{C17}$$

The constants A and B are again determined by matching the first and second derivatives of velocity at the interface. Thus

$$\begin{aligned} A &= \frac{\mu_o u_o''}{2} \\ B &= \frac{\mu_o u_o'}{2} \end{aligned} \tag{C18}$$

At the body $\partial u/\partial x$ vanishes, and solving for the coordinate x_b from equation (C17) results in

$$x_b = +\frac{\mu_o u_o''}{2\left(\frac{\partial^2 p}{\partial r^2}\right)}\left(1 - \sqrt{1 + \frac{4\partial^2 p}{\partial r^2}\frac{u_o'}{\mu_o u_o''}}\right) \tag{C19}$$

In Appendix B it is shown that

$$\frac{\partial^2 p}{\partial r^2} = -\frac{8}{\gamma_s + 1}\frac{\rho_\infty U_\infty^2}{R_s^2} \tag{C20}$$

Thus from equations (C13), (C14), and (C20), it can be shown that

$$4\frac{\partial^2 p}{\partial r^2}\frac{u_o'}{\mu_o u_o''^2} = \frac{(\gamma - 1)^2\sqrt{2(\gamma - 1)}}{(3 - 2\gamma)^2}\frac{\mu_\infty}{\mu_o}\frac{R_s}{R_b}\,Re_\infty \tag{C21}$$

which is large compared to unity for any reasonably large value of Reynolds number (of the order of hundreds or greater). Therefore, if

quantities of the order of unity are neglected in equation (C19), the stagnation point coordinate reduces to

$$x_b^2 = \frac{2\mu_o}{\sqrt{-\rho \frac{\partial^2 p}{\partial r^2}}} \tag{C22}$$

which is identical in form to the relation for body surface coordinate in the two-dimensional flow (eq. (19)).

Next, in region 1 the viscous dissipation and heat-conduction terms are again neglected in the energy equation, and terms that vanish by reasons of symmetry along the stagnation streamline are dropped. Thus the energy equation for region 1 takes the same form as equation (23) for the two-dimensional problem and, since the interface velocity is small, the interface temperature T_o is again approximately the stagnation temperature T_t.

In region 2, the heat-conduction terms in the energy equation predominate, and the equation reduces to the three-dimensional Laplace equation in the variable η

$$\frac{\partial^2 \eta}{\partial x^2} + \frac{\partial^2 \eta}{\partial y^2} + \frac{\partial^2 \eta}{\partial z^2} = 0 \tag{C23}$$

In order to fit the boundary conditions on a spherical surface, the solution is given in terms of spherical coordinates ($\bar{r}$, θ, and φ). The general solution which preserves symmetry about the x axis (i.e., which is independent of φ) is

$$\eta = A + \frac{B}{\bar{r}} + \sum_{n=1}^{\infty} \left(C_n \bar{r}^{-n} + \frac{D_n}{\bar{r}^{n+1}} \right) P_n(\cos \theta) \tag{C24}$$

where $P_n(\cos \theta)$ is the nth order Legendre polynomial in $\cos \theta$. If it is required that η be a constant, η_b, on the surface of the body, equation (C24) can be reduced, on the stagnation streamline, to

$$\eta = \eta_b - \frac{B}{R_b} \left(1 - \frac{R_b}{\bar{r}} \right) + \sum_{n=1}^{\infty} C_n \bar{r}^{-n} \left[1 - \left(\frac{R_b}{\bar{r}} \right)^{2n+1} \right] \tag{C25}$$

then expanding in terms of $\epsilon = \frac{\bar{r}}{R_b} - 1 << 1$, results in

$$\eta = \eta_b + L(\epsilon - \epsilon^2) + \cdots \tag{C26}$$

where L is $-\frac{B}{R_b} + \sum_{n=1}^{\infty} C_n(2n + 1)R_b^n$. Neglecting the quadratic term in ϵ, evaluating η at the interface, and transforming to the variable x, one obtains for equation (C26) on the stagnation streamline

$$\eta = \eta_o - (\eta_o - \eta_b)\frac{x}{x_b} \tag{C27}$$

Then the rate of heat transfer to the stagnation point is

$$-\eta_b' = \frac{\eta_o - \eta_b}{x_b} = \frac{1}{x_b}\int_{T_b}^{T_o} k\, dT \tag{C28}$$

which is identical in form with the zero-yaw solution for the two-dimensional-flow problem (eq. (31)). Note, however, that the second derivative of pressure given by equation (B18) is larger by a factor of 4/3 than it is for the corresponding two-dimensional-flow case with the same shock-wave curvature (eq. (B17)). Thus x_b given by equation (C22) is changed by the factor $(3/4)^{1/4}$ and the rate of heat transfer to an axially symmetric region becomes

$$-\eta_b' = \left[\frac{1}{2(\gamma_s - 1)}\right]^{1/4}\left(\frac{\mu_\infty}{\mu_o}\frac{R_b}{R_s}\right)^{1/2}\frac{Re_\infty^{1/2}}{R_b}\int_{T_b}^{T_o} k\, dT \tag{C29}$$

while the corresponding expression for Nusselt number is

$$Nu = \left(\frac{8}{\gamma_s - 1}\right)^{1/4}\left(\frac{\mu_\infty}{\mu_o}\frac{R_b}{R_s}\right)^{1/2}\frac{Re_\infty^{1/2}}{k_o(T_o - T_b)}\int_{T_b}^{T_o} k\, dT \tag{C30}$$

APPENDIX D

EXAMINATION OF ANALYTICAL RESULTS AND ASSUMPTIONS

A number of assumptions have been made in the theoretical analysis, and it is desirable now to show that the solutions obtained are both realistic and consistent with these assumptions. In particular, it will be shown that the presumption of a constant second derivative of pressure normal to the stagnation streamline yields solutions for the distance between shock wave and body which are reasonably close to observed values. Secondly, it will be demonstrated that the u velocity throughout region 2 is indeed small, as assumed in the analysis, if the Reynolds number is large enough for continuum flow conditions. In addition, it will be shown that for region 2 the viscous-dissipation terms due to the u and v component velocity derivatives are small compared to the heat-conduction terms in the energy equation, again provided the Reynolds number is not too small. These findings, then, help to justify the manner in which the momentum and energy equations were treated in the analysis.

Now it is obvious that the assumption of an abrupt transition from nonviscous, convective flow to viscous, conductive flow is a substantial idealization of the actual flow.[1] It is possible, however, to make a gross check on the self-consistency of this model by comparing the amount of heat convected across the interface with the amount conducted to the body surface. When this is done it is found that from a heat-flow point of view, the model is self-consistent (i.e., heat convected provides for heat conducted).

As a final point, a comparison will be made between the analysis of this paper and the heat-transfer solutions for low-velocity flow given by Howarth (ref. 7) and Cohen and Reshotko (ref. 8).

Distance Between Shock Wave and Body

Consider first axially symmetric flow. The velocity in region 1 was found to be (eq. (C10))

$$u = u_o + u_o' x + \frac{u_o''}{2} x^2 \qquad (D1)$$

[1]Strictly speaking, this idealized model should be considered simply a first approximation to the correct situation. A second approximation would be to divide the domain between the body and shock wave into three regions rather than two as was done here.

Then, the shock-wave coordinate must be

$$x_s = \frac{u_s' - u_o'}{u_o''} \tag{D2}$$

It can be shown from the relations in Appendix B and equations (C11) and (C12) that

$$\left.\begin{aligned} u_s' &= -\frac{4U_\infty}{(\gamma_s + 1)R_s} \\ u_o' &= -\sqrt{-\frac{4}{\rho}\frac{\partial^2 p}{\partial r^2}} = -\frac{4U_\infty}{(\gamma_s + 1)R_s}\sqrt{2(\gamma_s - 1)} \\ u_o'' &= \frac{8(3 - 2\gamma)}{\gamma_s^2 - 1}\frac{U_\infty}{R_s^2} \end{aligned}\right\} \tag{D3}$$

Substituting these relations into equation (D2) yields

$$\frac{x_s}{R_s} = -\frac{(\gamma_s - 1)\left[1 - \sqrt{2(\gamma_s - 1)}\right]}{2(3 - 2\gamma_s)} \tag{D4}$$

Note that for $\gamma_s = 1.5$, u_o'' vanishes and the velocity profile becomes linear. For this case x_s/R_s reduces to $(\gamma_s - 1)/4$.

The actual distance between the body and the shock wave is, of course, the sum of x_s and x_b. However, it can be shown from equations (C22) and (D4) that x_b is small compared to x_s for reasonably large Reynolds numbers, and x_b will therefore be neglected. The ratio x_s/R_s calculated from equation (D4) for γ_s equal 1.4 is 0.105. Measurements of x_s/R_b taken from spark photographs of high-velocity spheres presented by Charters and Thomas (ref. 15) and Dugundji (ref. 16) approach this value closely at high Mach numbers (i.e., x_s/R_b about 0.11 at Mach number 4). Heybey (ref. 17) has developed a theory which fits the data of references 15 and 16 closely and, for the limit of infinite Mach number, predicts x_s/R_b about 0.12. Thus it is seen that at high Mach numbers, the assumption that the second derivative of pressure is constant and that the ratio R_b/R_s is near unity yields results which are consistent with experimentally observed distances between shock wave and body, as well as with the theory of Heybey.

It is of interest to calculate the shock-wave coordinate for two-dimensional flow as well. Recall that the solution for velocity in region 1 for this case is

$$u = \frac{u_o'}{C} \sinh Cx \tag{D5}$$

and thus

$$\frac{\partial u}{\partial x} = u_o' \cosh Cx$$

The velocity derivatives at the shock wave and at the interface, given in Appendix B, are, respectively,

$$\left.\begin{aligned} u_s' &= -\frac{2U_\infty}{(\gamma_s + 1)R_s} \\ u_o' &= -\sqrt{-\frac{1}{\rho}\frac{\partial^2 p}{\partial y^2}} = -\frac{U_\infty\sqrt{6(\gamma_s - 1)}}{(\gamma_s + 1)R_s} \end{aligned}\right\} \tag{D6}$$

Then the product Cx_s is given by

$$Cx_s = \operatorname{arc\,cosh} \frac{2}{\sqrt{6(\gamma_s - 1)}} \tag{D7}$$

With Cx_s known and the velocity at the shock wave

$$u_s = \frac{\gamma_s - 1}{\gamma_s + 1} U_\infty \tag{D8}$$

The shock-wave coordinate becomes

$$\frac{x_s}{R_s} = -\sqrt{\frac{\gamma_s - 1}{6}} \frac{Cx_s}{\sinh Cx_s} \tag{D9}$$

For a γ_s of 1.4, Cx_s takes the value 0.75 and since the sinh function is very nearly linear over this range, rather close bounds on the shock-wave coordinate are imposed by

$$\left|\frac{u_s}{u_s'}\right| < \left|x_s\right| < \left|\frac{u_s}{u_o'}\right| \tag{D10}$$

or

$$\frac{\gamma_s - 1}{2} < \left|\frac{x_s}{R_s}\right| < \sqrt{\frac{\gamma_s - 1}{6}} \tag{D11}$$

The exact theoretical solution for x_s/R_s at $\gamma_s = 1.4$ is 0.236. According to the theory then, a shock wave with given radius of curvature should be detached from a cylindrical body about twice as far as from a sphere.

Magnitude of Velocity in Region 2

The y momentum equation in region 2 was reduced to

$$\mu \frac{\partial u}{\partial x} = - \frac{\partial^2 p}{\partial y^2} \frac{x^2}{2} + \mu_o u_o' \tag{D12}$$

The left side of this equation may be approximated by $\frac{\partial}{\partial x}(\mu u)$ with the presumption that velocity in region 2 is small. Then equation (D12) may be integrated to

$$\mu u = - \frac{\partial^2 p}{\partial y^2} \frac{x^3}{6} + \mu_o u_o' x + \mu_o u_o \tag{D13}$$

Solving for u_o, noting that velocity vanishes at x_b, and substituting from equations (14) and (19), one obtains

$$u_o = - \frac{2}{3} u_o' x_b = \frac{2}{3} \sqrt{- \frac{2\mu_o u_o'}{\rho_s}} \tag{D14}$$

It follows that the ratio of interface velocity to the velocity at the shock wave is given by

$$\left(\frac{u_o}{u_s}\right)^2 = -\frac{8}{9}\frac{\mu_o}{\rho_s u_s}\frac{u_o'}{u_s} = -\frac{16}{9}\left(\frac{\mu_o}{\mu_\infty}\right)\frac{R_b}{Re_\infty}\frac{u_o'}{u_s} \tag{D15}$$

which on substituting the relations given in Appendix B for u_o' and u_s becomes

$$\left(\frac{u_o}{u_s}\right)^2 = \frac{16}{9}\sqrt{\frac{6}{\gamma_s - 1}}\left(\frac{\mu_o}{\mu_\infty}\frac{R_b}{R_s}\right)\frac{1}{Re_\infty} \tag{D16}$$

It can be seen that for large Reynolds numbers, of the order of hundreds or greater, the velocity at the interface is small compared to the velocity at the shock wave. Since the velocity in region 2 is everywhere less than at the interface (see eq. (D13)), the solutions obtained for velocity are consistent with the assumption that velocity is small throughout region 2.

Viscous Dissipation in Region 2

Although the derivative of velocity vanishes at the body surface, it increases parabolically (see eq. (D12)) to u_o' at the interface. Since viscous dissipation terms due to this velocity shear were neglected in solving the energy equation, it will be shown that the maximum value of these terms, which occurs at the interface, is small compared to the heat-conduction terms like $\partial^2\eta/\partial x^2$ (note that by continuity $\partial v/\partial y$ contributes a dissipation term of the same magnitude as $\partial u/\partial x$). From equation (30) it can be seen that the term $\partial^2\eta/\partial x^2$ is nearly constant everywhere along the stagnation streamline in region 2. Then the ratio of differential terms in the energy equation is, by equations (30) and (D14),

$$\frac{4\mu_o(u_o')^2}{(\partial^2\eta/\partial x^2)_b} = \frac{9\mu_o u_o^2}{x_b} R_b \left(\int_{T_b}^{T_o} k\, dT\right)^{-1} \tag{D17}$$

If equation (D17) is evaluated for constant heat capacity and thermal conductivity proportional to the nth power of temperature, there is obtained

$$\frac{4\mu_o(u_o')^2}{(\partial^2\eta/\partial x^2)_b} = 18(n+1)\left(\frac{u_o}{U_\infty}\right)^2 Pr\left(\frac{R_b}{x_b}\right) \tag{D18}$$

Substituting for velocity ratio u_o/U_∞ from equations (D16) and (B4) and for the ratio R_b/x_b from equation (21), there results

$$\frac{4\mu_o(u_o')^2}{(\partial^2\eta/\partial x^2)_b} = 16(n+1)\mathrm{Pr}\left(\frac{\gamma-1}{\gamma+1}\right)^2\left(\frac{6}{\gamma-1}\right)^{3/4}\left(\frac{\mu_o}{\mu_\infty}\right)^{1/2}\left(\frac{R_b}{R_s}\right)^{3/2}\mathrm{Re}_\infty^{-1/2} \qquad \text{(D19)}$$

Once again the square root of Reynolds number is the predominant term for conditions of continuum flow and thus the viscous dissipation terms in the energy equation are small compared to the conduction terms in region 2.

Heat Convection Across the Interface, x = 0

Next consider the ratio of the heat convected across the interface, $\rho u_o \int_o^{T_o} C_p dT$, to the heat transfer at the stagnation point of the body, $-\eta_b'$. The value of u_o given by equation (D14) and $-\eta_b'$ from equation (32) yields

$$-\frac{\rho u_o}{\eta_b'}\int_o^{T_o} C_p dT = -\frac{2u_o' x_b^2 \rho}{3}\frac{\int_o^{T_o} C_p dT}{\int_{T_b}^{T_o} k\, dT} \qquad \text{(D20)}$$

Again evaluating for constant heat capacity and the nth power temperature function for thermal conductivity, and noting from equations (14) and (19) that $u_o' x_b^2$ reduces to $-(2\mu_o/\rho)$, one obtains

$$-\frac{\rho u_o C_p T_o}{\eta_b'} = \frac{4}{3}\mathrm{Pr}(n+1) \qquad \text{(D21)}$$

This ratio is the order of unity, and thus the right magnitude of heat is convected across the interface to balance the heat conducted to the body. The above result also provides a check on the value of x_b which was obtained by matching u_o' as a boundary condition of the y momentum equation.

Low-Velocity Heat Transfer

For hypersonic velocities it was found that taking shock-wave curvature equal to body curvature on the stagnation streamline gave approximately the correct answer for the distance between the body and the shock wave, so presumably the ratio R_b/R_s should be taken near unity when calculating the heat transfer as well. Undoubtedly this ratio will be somewhat less than unity for low Mach number supersonic flow, and it is of interest to see what the solutions developed in this paper will predict for this case (even though the assumptions made in the analysis are not expected to hold as well for the low-velocity flow conditions). For this purpose it is convenient to express the body coordinate x_b in terms of $(\partial v/\partial y)_o$ which by continuity equals $-u_o'$. From equations (9), (14), and (19)

$$x_b = \sqrt{\frac{2\mu_o}{\rho(\partial v/\partial y)_o}} \tag{D22}$$

then solving for Nusselt number from equations (32) and (34) for the case of the cool wall ($T_b/T_o << 1$, and $n = 1/2$) one obtains

$$Nu = \frac{2}{3}\frac{D_b}{x_b} = 0.47\, D_b \sqrt{\frac{\rho(\partial v/\partial y)_o}{\mu_o}} \tag{D23}$$

The method of boundary-layer solution for low-velocity flow about a cylinder given in reference 7, yields for the derivative of velocity component normal to the stagnation streamline at the edge of the boundary layer, in the notation of this paper,

$$\left(\frac{\partial v}{\partial y}\right) = \frac{3.8U_s}{D_b} \tag{D24}$$

Substituting in equation (D23) results in

$$Nu = 0.92\, Re_s^{1/2}$$

where the small differences between μ_s and μ_o are neglected. The constant 0.92 compares favorably with the value 0.95 given by Howarth for $Pr = 0.72$. This agreement is especially remarkable in the light of the fact that the analysis of reference 7 is for constant thermal properties, while variation in thermal properties is an essential feature of this analysis.

Cohen and Reshotko (ref. 8) find that the solution for a compressible boundary layer gives the following relation at the stagnation point of an axially symmetric body

$$\frac{Nu\ y}{D_b} = 0.440 \sqrt{\frac{\rho v y}{\mu}} \tag{D25}$$

for the case of a cool wall and a Prandtl number 0.7. If the radial component of velocity v is taken proportional to y, the ordinate can be eliminated and equation (D25) reduces to

$$Nu = 0.440\ D_b \sqrt{\frac{\rho(\partial v/\partial y)_o}{\mu}} \tag{D26}$$

The factor 0.440 given by Cohen and Reshotko compares favorably with the factor 0.47 given in equation (D23).

APPENDIX E

ESTIMATE OF RESERVOIR TEMPERATURES IN THE HYPERSONIC GUN TUNNEL

A highly nonisentropic compression process, like the multiple reflection of shock waves that occurs in the reservoir section of the hypersonic gun tunnel, is capable of producing high final air temperatures. An estimate of the magnitude of the reservoir temperatures attainable in the gun tunnel is obtained by equating the internal energy gained by the reservoir air to the work done in compressing this air. Thus assuming no heat loss (i.e., adiabatic compression) we have

$$\rho_1 V_1 \int_{T_1}^{T_2} C_V dT = - \int_{V_1}^{V_2} p \, dV \tag{E1}$$

where the subscripts 1 and 2 refer to conditions before and after the compression, V is the volume of the gas, and C_V is the specific heat at constant volume. In terms of an average specific heat, $\overline{C_V}$, and a mean pressure, $\bar{p}$, equation (E1) is

$$\rho_1 V_1 \overline{C_V}(T_2 - T_1) = \bar{p}(V_1 - V_2) \tag{E2}$$

By substitution of the mass conservation relation, $\rho_1/\rho_2 = V_2/V_1$, the ideal gas law $p = \rho RT$, and an average ratio of specific heats $\bar{\gamma}$ defined by $\bar{\gamma} - 1 = R/\overline{C_V}$, equation (E2) can be transformed to

$$\frac{T_2}{T_1} = \frac{1 + (\bar{\gamma} - 1)\bar{p}/p_1}{1 + (\bar{\gamma} - 1)\bar{p}/p_2} \tag{E3}$$

Now the mean pressure during the compression process will probably be less than the final pressure, p_2, but greater than the average $(p_1 + p_2)/2$. If these values are taken as the limits of $\bar{p}$, and in addition p_1 is very small compared to p_2, the temperature limits given by equation (E3) become approximately

$$\frac{\bar{\gamma} - 1}{\bar{\gamma} + 1}\frac{p_2}{p_1} \leq \frac{T_2}{T_1} \leq \frac{\bar{\gamma} - 1}{\bar{\gamma}}\frac{p_2}{p_1} \tag{E4}$$

For an average ratio of specific heats $\bar{\gamma} = 1.3$, the limits become

$$0.13 \frac{p_2}{p_1} \leq \frac{T_2}{T_1} \leq 0.23 \frac{p_2}{p_1} \tag{E5}$$

The compression ratio realized in the hypersonic gun tunnel is presently about 32. Then for an initial temperature $T_1 = 530^\circ$ R, the reservoir temperature limits indicated by equation (E5) are

$$2200^\circ \text{ R} \leq T_2 \leq 3900^\circ \text{ R} \tag{E6}$$

Recall that the reservoir temperature deduced from the velocity measurements is 2200° R, the lower limit given by equation (E6). Undoubtedly the temperature corresponding to no heat loss from the reservoir would be somewhat higher than this, however. It is interesting to note that an isentropic compression of the same value, with no heat losses, would yield a final reservoir temperature T_2 of only 1180° R.

APPENDIX F

PROBLEMS IN CONNECTION WITH CALIBRATING THE HYPERSONIC GUN TUNNEL

Static-Pressure Measurements

The static pressure system is considered to respond exponentially to the true static pressure which is in turn assumed to be proportional to the pitot pressure. In this event we may write

$$\frac{dp}{dt} = \frac{1}{\tau}(Kp_t - p) \tag{F1}$$

where τ is the time constant of the system, and K is the ratio of static to pitot pressure. By integration of equation (F1), the constants τ and K stand in the linear relation

$$\frac{\int_o^t p\,dt}{p(t) - p(o)} = K\left[\frac{\int_o^t p_t dt}{p(t) - p(o)}\right] - \tau \tag{F2}$$

The above integrals of pressure are evaluated as a function of time from the measured static-pressure and pitot-pressure data. Then the values of K and τ are determined by the linear regression giving the least mean squares fit. It was found (see fig. 13) that a time constant $\tau = 0.060$ second and a ratio of static to pitot pressure $K = 8.06\times10^{-3}$ fit the pressure data shown in figures 5(c) and 5(d) within a few percent over the entire interval of flow time from 0 to 0.3 second. Accordingly, it is indicated that the value of p/H, corrected for time lag in the static pressure measuring system, is 5.32×10^{-6} over this time interval.

Condensed Phase Impurities

It was observed during the course of experimenting with the hypersonic gun tunnel that the condensed phase impurities are absent from the shadow of models in the air stream. This observation suggests that the energy carried to a model by these impurities may vary in proportion to the frontal area of the model. In this event, the heat transfer should

tend to vary directly as the Reynolds number for the case of circular cylinders in the same stream. However, according to both theory and experiment (see fig. 9) heat transfer varies like the square root of Reynolds number. There is added reason, then, to believe that condensed phase impurities have but a small influence on the initial heat-transfer rates presented in this paper.

APPENDIX G

EFFECTS OF DISSOCIATION ON HEAT TRANSFER TO A CYLINDRICAL STAGNATION REGION

Temperatures in the disturbed flow about a vehicle in hypersonic flight may be sufficiently large (of the order of 5000° R or greater) to dissociate air molecules into atoms. Rates of dissociation are not presently known with any degree of certainty, however, and it is therefore difficult to estimate whether the extent of dissociation will be negligible, partial, or in complete equilibrium in the time scale of flow about hypersonic vehicles of practical size. Since equilibrium dissociation is a limiting case, it is this situation which will be treated here.

To a first approximation then, the temperature ratio across the shock wave is determined by the relation

$$h_s = \frac{U_\infty^2}{2} = \frac{\gamma_\infty R(T_\infty) T_\infty M_\infty^2}{2} \tag{G1}$$

since the specific enthalpy, h_s, is considered a known function of temperature for a given pressure. If the free-stream static pressure is neglected, the momentum equation becomes

$$p_s + \rho_s u_s^2 = \rho_\infty U_\infty^2 \tag{G2}$$

and substituting from the continuity relation

$$\rho_s u_s = \rho_\infty U_\infty \tag{G3}$$

and the equation of state

$$p = \rho R(T) T \tag{G4}$$

the ratio of densities across the shock wave becomes

$$\frac{\rho_\infty}{\rho_s} = \frac{1}{2} - \sqrt{\frac{1}{2} - \frac{R(T_s)}{U_\infty^2}} \tag{G5}$$

Then if γ_s is defined by[1]

$$\frac{\rho_\infty}{\rho_s} = \frac{\gamma_s - 1}{\gamma_s + 1} \tag{G6}$$

the pressure ratio across the shock wave is

$$\frac{p_s}{p_\infty} = \frac{2\gamma_\infty M_\infty^2}{\gamma_s + 1} \tag{G7}$$

From the equation of state (G4) and equation (G6), it follows that an equivalent expression is

$$\frac{p_s}{p_\infty} = \frac{\gamma_s + 1}{\gamma_s - 1} \frac{T_s}{T_\infty} \frac{R(T_s)}{R(T_\infty)} \tag{G8}$$

where the ratio of specific gas constants $R(T_s)/R(T_\infty)$ is also considered a known function of temperature for a given pressure. Equations (G7) and (G8) are solved for γ_s; then the rate of heat transfer to a cylindrical stagnation region may be calculated from equation (33). Note that it is unnecessary to determine γ_s with great precision, since it is the fourth root of $(\gamma_s - 1)$ which appears in equation (33).

The above calculations were made for a cylindrical stagnation region for the case of equilibrium dissociation at one atmosphere pressure and

[1]This definition is used merely for convenience, so that the constants given in the heat-transfer solution (eq. (33)) do not change in form.

free-stream temperature, T_∞, equal 400° R.[2] The enthalpy and specific gas constants were taken from data tabulated by Kreiger and White (ref. 18) and the transport properties were approximated by simple kinetic theory relations for a gas composed of hard spherical particles (see ref. 19). The quantitative accuracy of this approximation is not high, of course, and the analysis cannot be expected to yield more than the order of magnitude for dissociation effects. The results of these calculations are presented in figure 12 both for flow in a state of equilibrium dissociation and for flow in which dissociational energy is not excited. The calculated rates of heat transfer are higher when dissociation occurs but not in proportion to the large order of magnitude increase in transport properties. The explanation for this result is that the increase in transport properties is largely compensated for by a reduction in temperature level as the random kinetic energy is absorbed in the dissociational energy modes. In fact, as a result of this compensation, Beckwith concludes on the basis of a boundary-layer analysis (ref. 20), that the heat-transfer rate per unit area at the stagnation point is only slightly affected by equilibrium dissociation. A close comparison of the results of this paper with Beckwith's results would not seem warranted until the properties of dissociated air are more accurately known.

[2]These conditions correspond roughly to upper atmosphere flight conditions (i.e., about 100,000 to 150,000 feet altitude at Mach numbers from 10 to 20). At lower altitudes, higher pressures will be encountered behind the shock wave and the equilibrium dissociation will be less. It should be remembered, of course, that equilibrium dissociation may not occur in actual flight if the rate process is slow enough (see, e.g., ref. 21 for a discussion of dissociation rates).

REFERENCES

1. Allen, H. Julian, and Eggers, A. J., Jr.: A Study of the Motion and Aerodynamic Heating of Missiles Entering the Earth's Atmosphere at High Supersonic Speeds. NACA RM A53D28, 1953.

2. Eggers, Alfred J., Jr., Allen, H. Julian, and Neice, Stanford E.: A Comparative Analysis of the Performance of Long-Range Hypervelocity Vehicles. NACA RM A54L10, 1955.

3. Eggers, A. J., Jr., Dennis, David H., and Resnikoff, Meyer M.: Bodies of Revolution for Minimum Drag at High Supersonic Airspeeds. NACA RM A51K27, 1952.

4. Sommer, Simon C., and Stark, James A.: The Effect of Bluntness on the Drag of Spherical-Tipped Truncated Cones of Fineness Ratio 3 at Mach Numbers 1.2 to 7.4. NACA RM A52B13, 1952.

5. Lamb, Horace: Hydrodynamics. Sixth ed., Dover Pub., 1945.

6. Stewart, H. J.: The Energy Equation for a Viscous Compressible Fluid. Nat. Acad. Sci., vol. 28, 1942, p. 161.

7. Howarth, L., ed.: Modern Developments in Fluid Dynamics, High Speed Flow. Oxford Clarendon Press, 1953.

8. Cohen, Clarence B., and Reshotko, Eli: Similar Solutions for the Compressible Laminar Boundary Layer with Heat Transfer and Pressure Gradient. NACA TN 3325, 1955.

9. Ames Research Staff: Equations, Tables and Charts for Compressible Flow. NACA Rep. 1135, 1953.

10. Eggers, A. J., Jr.: One-Dimensional Flows of an Imperfect Diatonic Gas. NACA Rep. 959, 1950. (Formerly NACA TN 1861)

11. Kovasznay, Leslie S. G.: The Hot-Wire Anemometer in Supersonic Flow. Jour. Aero. Sci., vol. 17, no. 9, 1950, pp. 565-572, 584.

12. Stine, Howard A.: Investigation of Heat Transfer from Hot Wires In the Transonic Speed Range. Heat Trans. and Fluid Mech. Inst., Berkeley, Calif., June 30 - July 2, 1954.

13. Stalder, Jackson R., Goodwin, Glen, and Creager, Marcus O.: Heat Transfer to Bodies in a High-Speed Rarified-Gas Stream. NACA Rep. 1093, 1952.

14. Sibulkin, M.: Heat Transfer Near the Forward Stagnation Point of a Body of Revolution. Jour. Aero. Sci., vol. 19, no. 8, 1952, pp. 570-571.

15. Charters, A. C., and Thomas, R. N.: The Aerodynamic Performance of Small Spheres from Subsonic to High Supersonic Velocities. Jour. Aero. Sci., vol. 12, no. 4, 1945, pp. 468-476.

16. Dugundji, John: An Investigation of the Detached Shock in Front of a Body of Revolution. Jour. Aero. Sci., vol. 15, no. 12, 1948, pp. 699-705.

17. Heybey, W. H.: Shock Distance in Front of Symmetrical Bodies. Naval Ordnance Lab., Rep. 3594, Dec. 24, 1953.

18. Krieger, F. J., and White, W. B.: The Composition and Thermodynamic Properties of Air at Temperatures from 500 to 8000° K and Pressures from 0.00001 to 100 Atmospheres. Rep. R-149, The Rand Corp., Apr. 15, 1949.

19. Hansen, C. Frederick: Note on the Prandtl Number for Dissociated Air. Jour. Aero. Sci., vol. 20, no. 11, 1953, pp. 789-790.

20. Beckwith, Ivan E.: The Effect of Dissociation in the Stagnation Region of a Blunt-Nosed Body. Jour. Aero. Sci., vol. 20, no. 9, 1953, pp. 645-646.

21. Glasstone, Samuel, Laidler, Keith J., and Eyring, Henry: The Theory of Rate Processes. McGraw Hill Book Co., Inc., 1941.

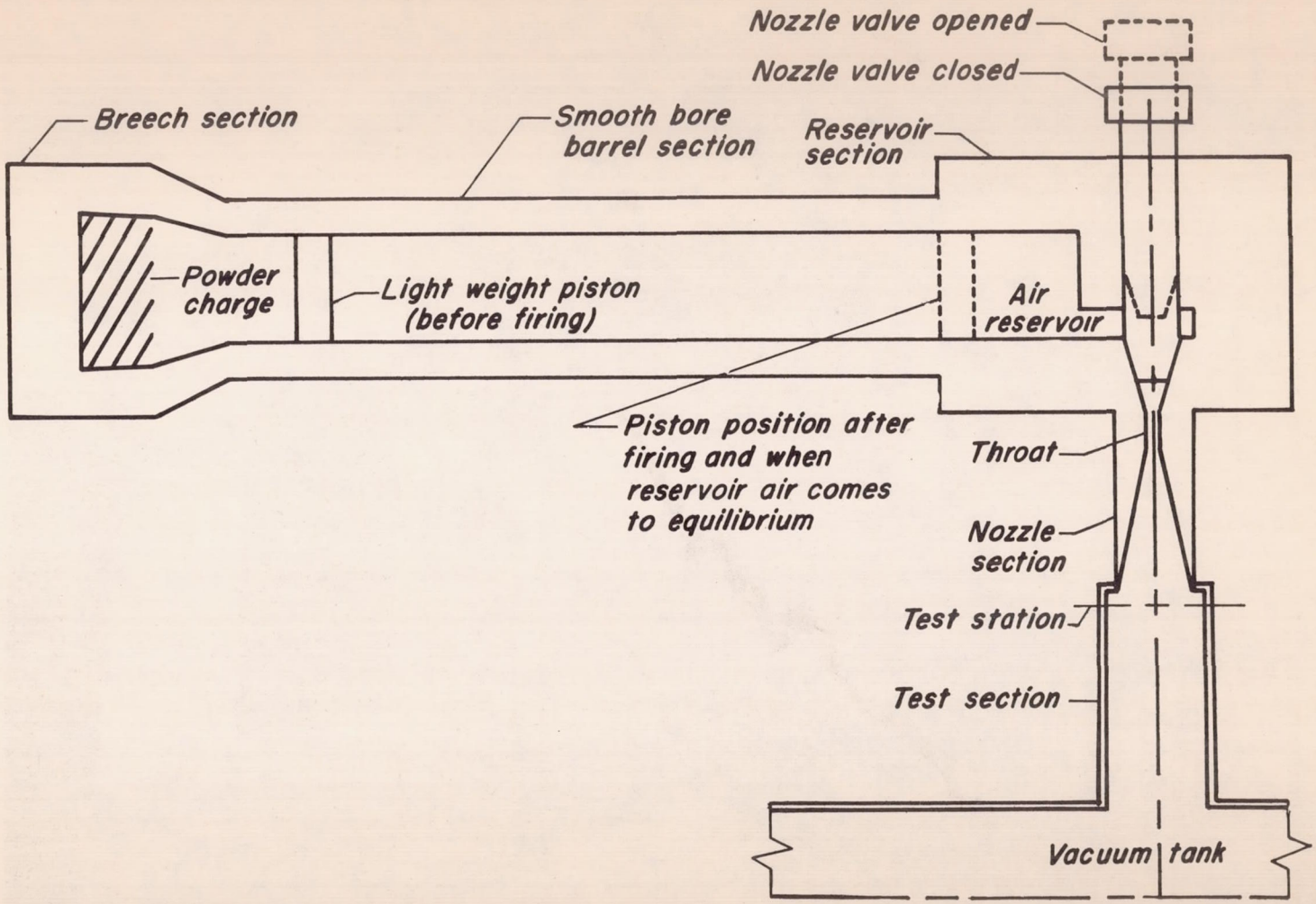

Figure 1.– Schematic diagram of the hypersonic gun tunnel.

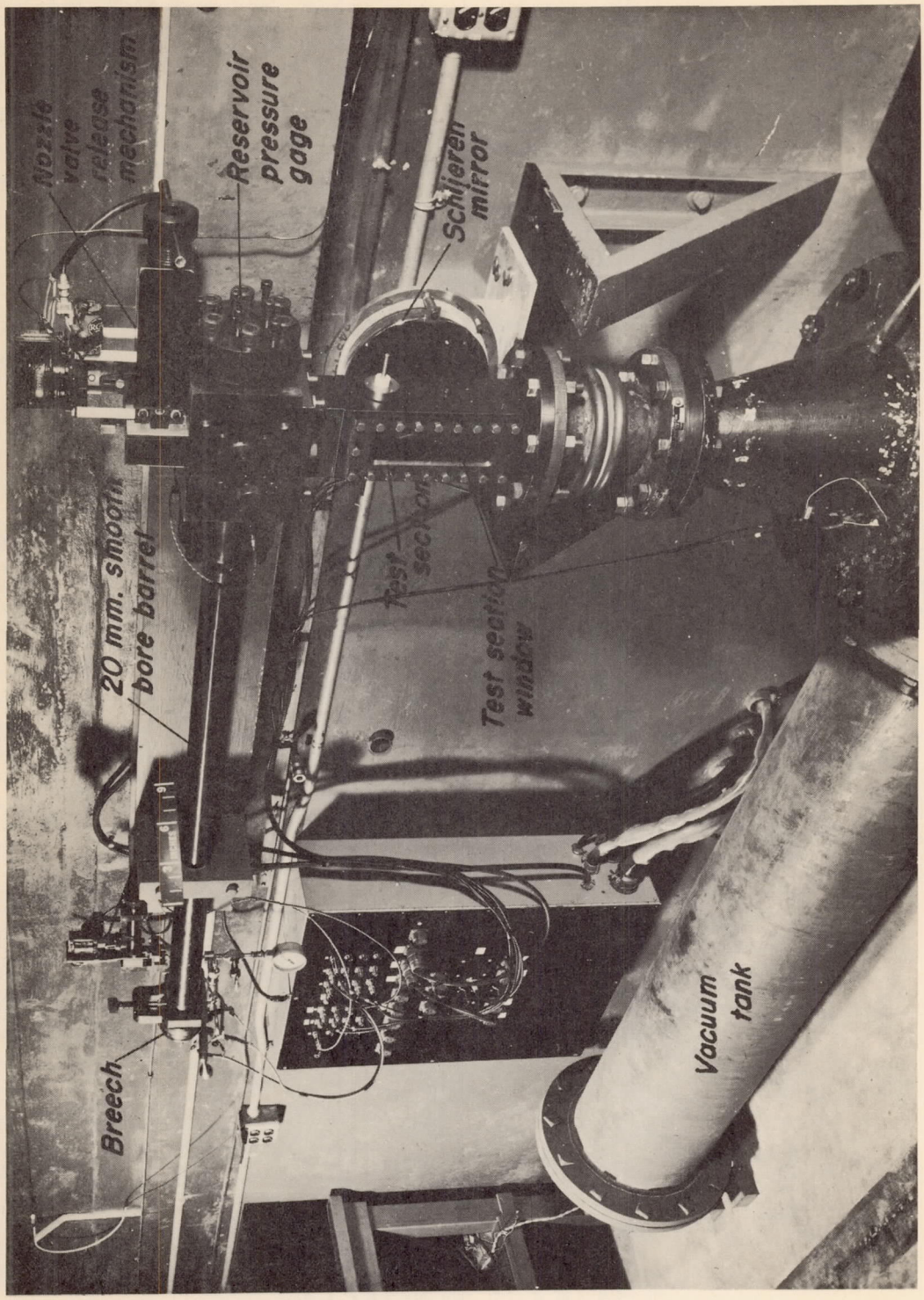

Figure 2.- 20-mm hypersonic gun tunnel.

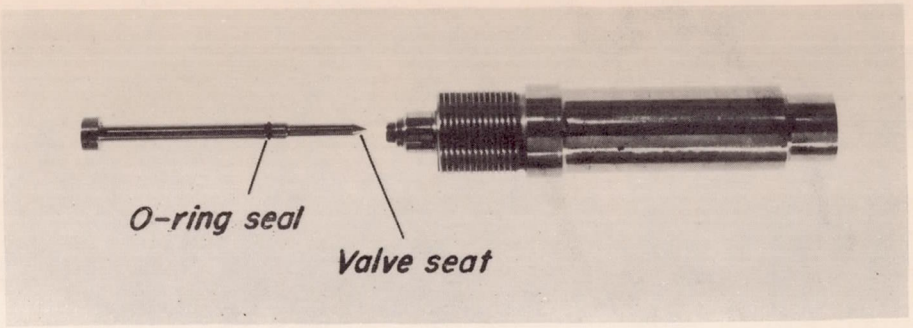

A-19912.1

(a) Photograph of nozzle valve and nozzle.

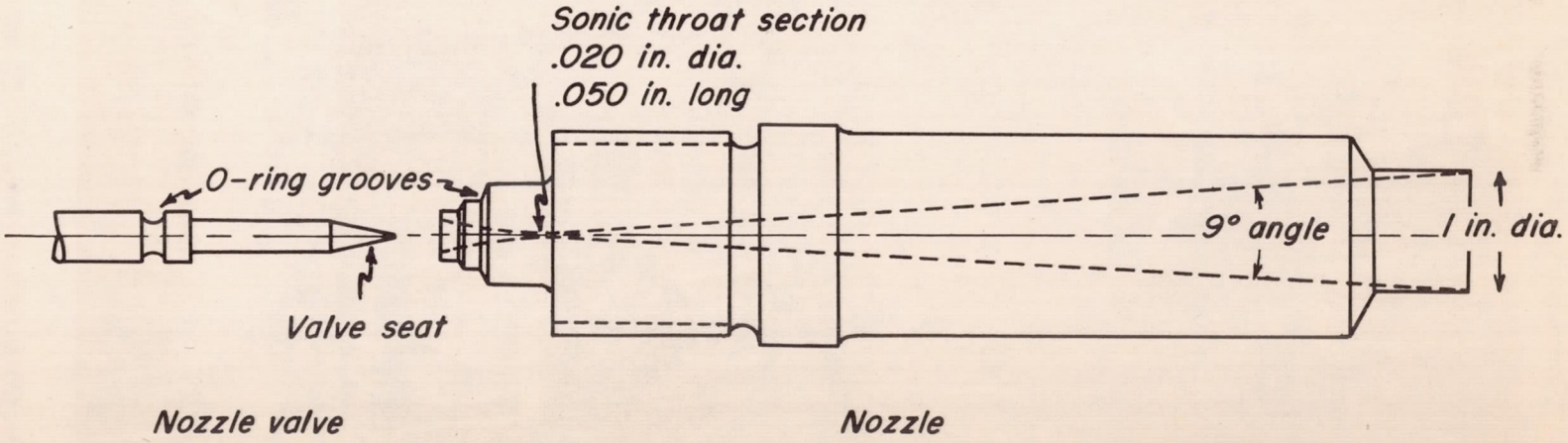

(b) Schematic diagram.

Figure 3.- Nozzle and nozzle valve for the 20-mm hypersonic gun tunnel.

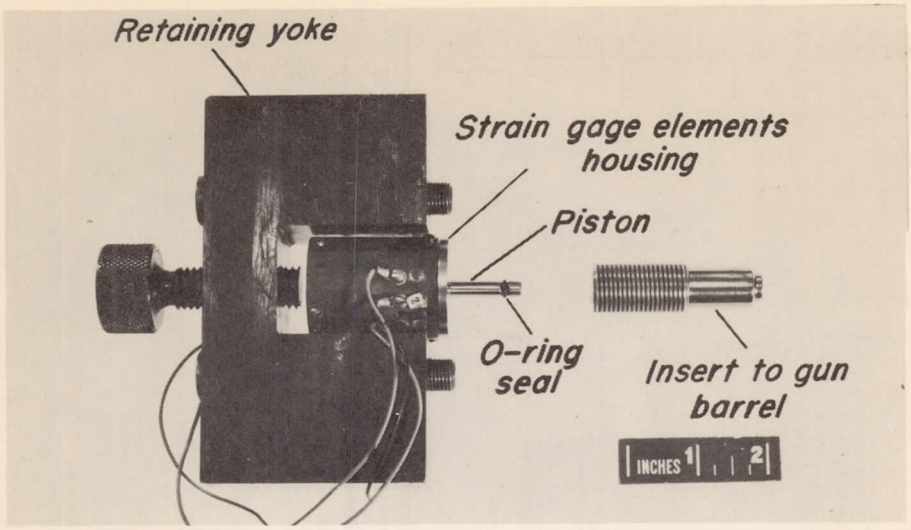

A-19913.1

(a) Reservoir pressure gage, gage insert, and yoke.

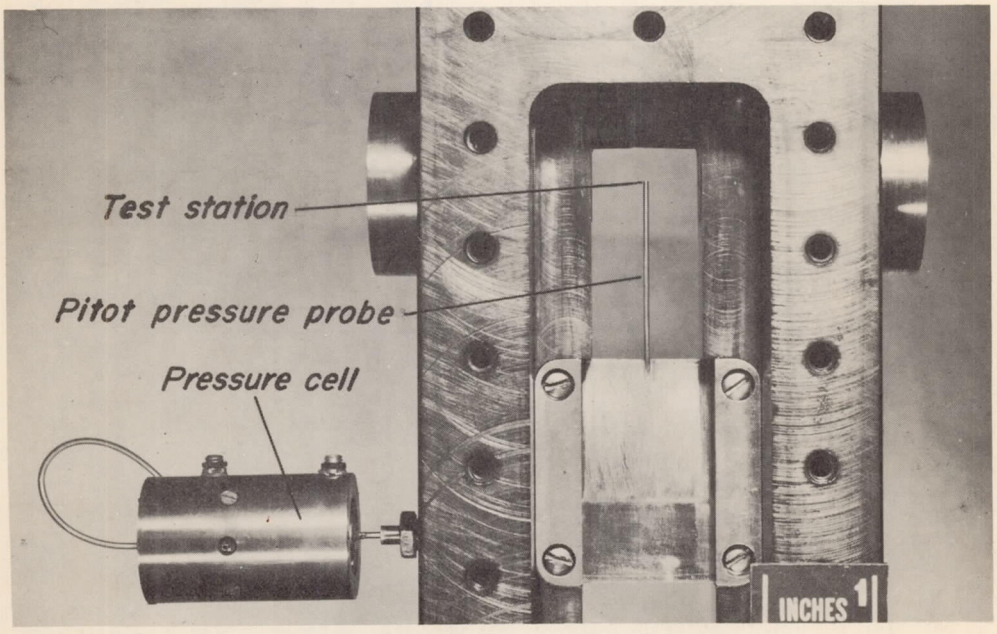

A-19914.1

(b) Pitot pressure probe and capacitance pressure cell.

Figure 4.– Calibration equipment for the 20-mm hypersonic gun tunnel.

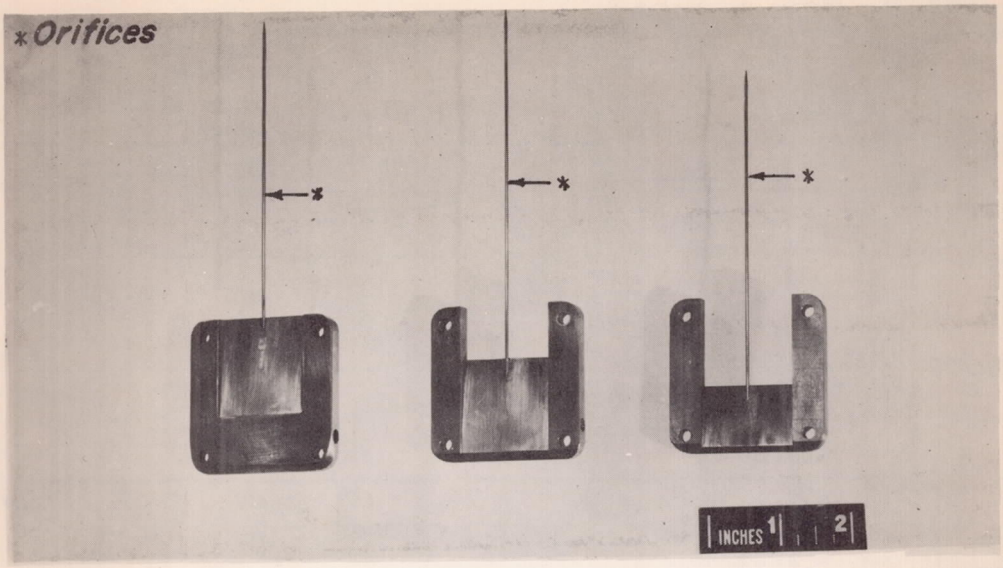

A-19915.1

(c) Static pressure probes

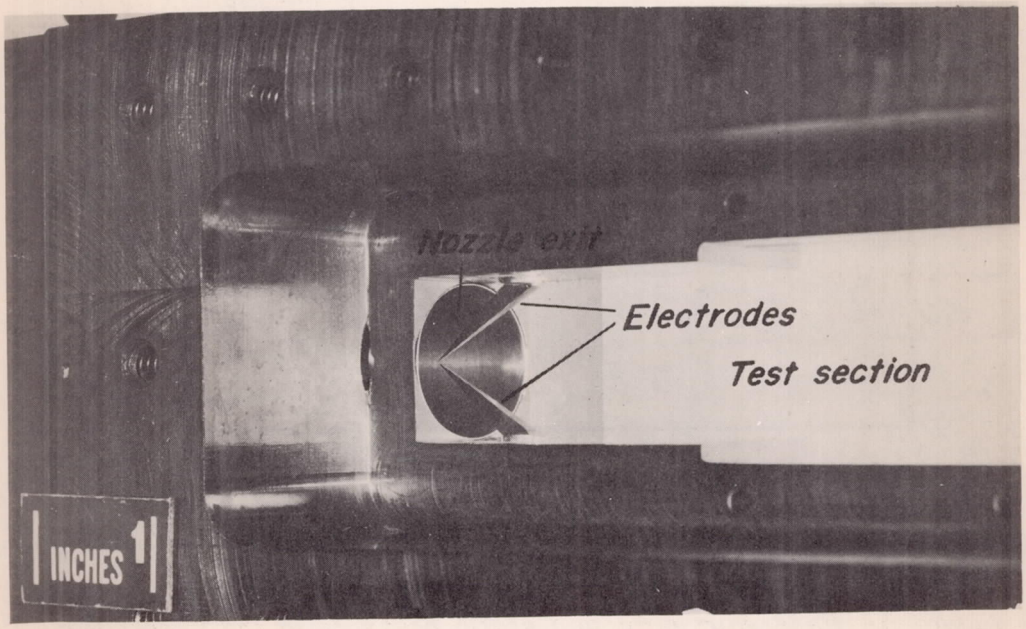

A-19916.1

(d) Spark electrodes mounted in test section

Figure 4.- Concluded.

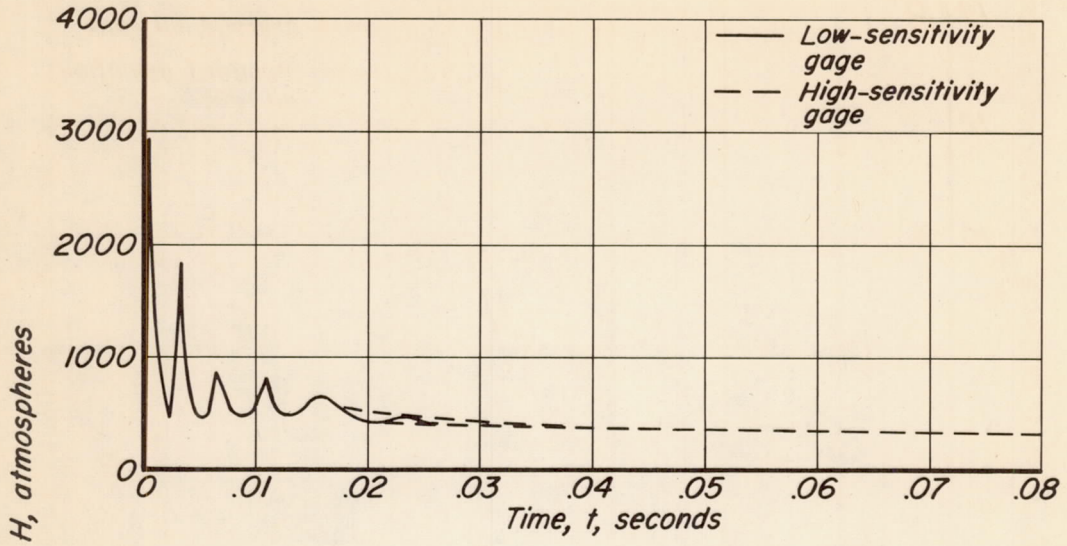

(a) Reservoir pressure, 0-0.08 seconds.

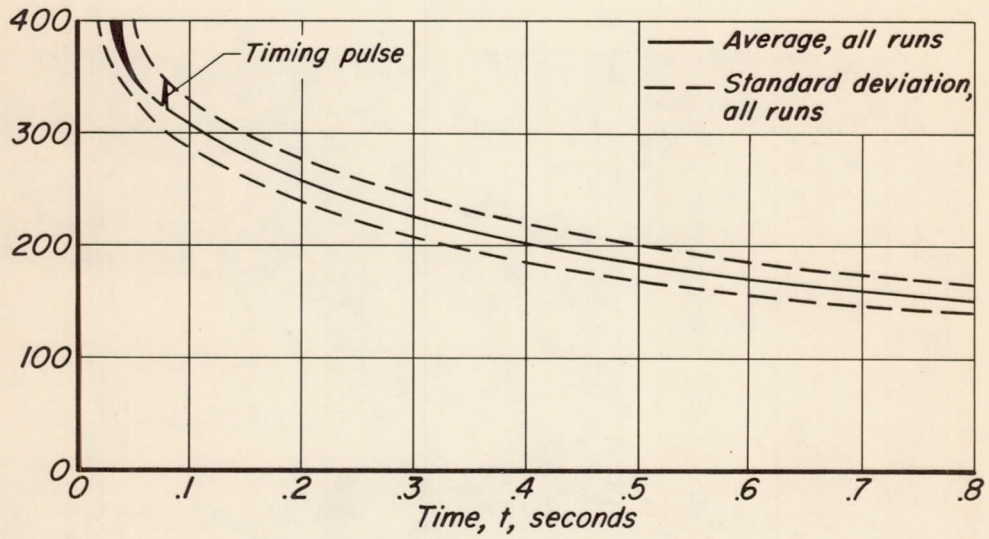

(b) Reservoir pressure, 0-0.8 seconds, taken with high-sensitivity gage.

Figure 5.- Reservoir, pitot and static pressure in the hypersonic gun tunnel as a function of time.

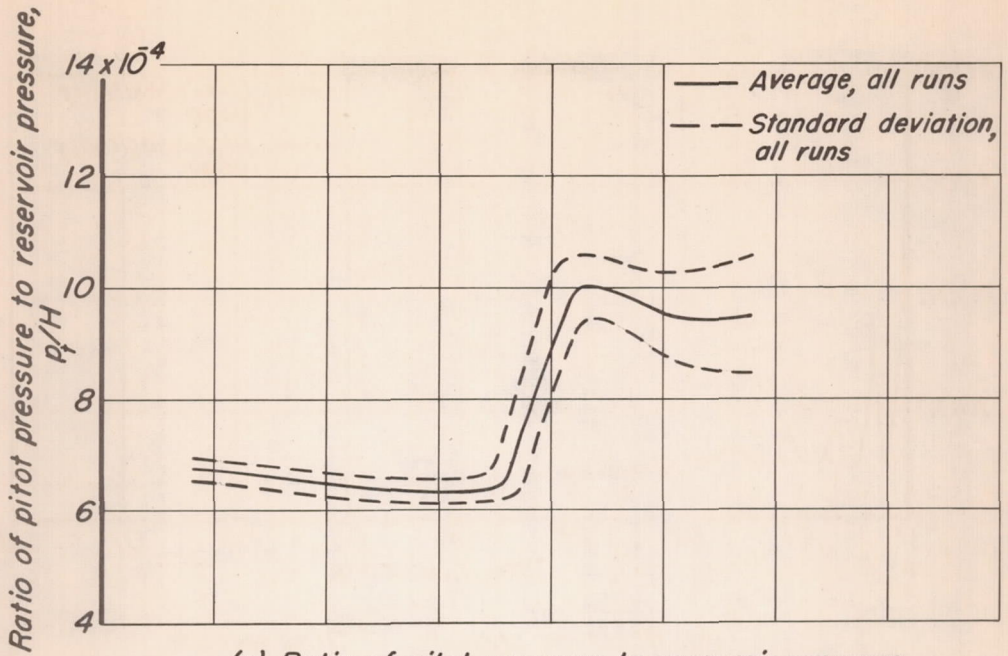

(c) Ratio of pitot pressure to reservoir pressure.

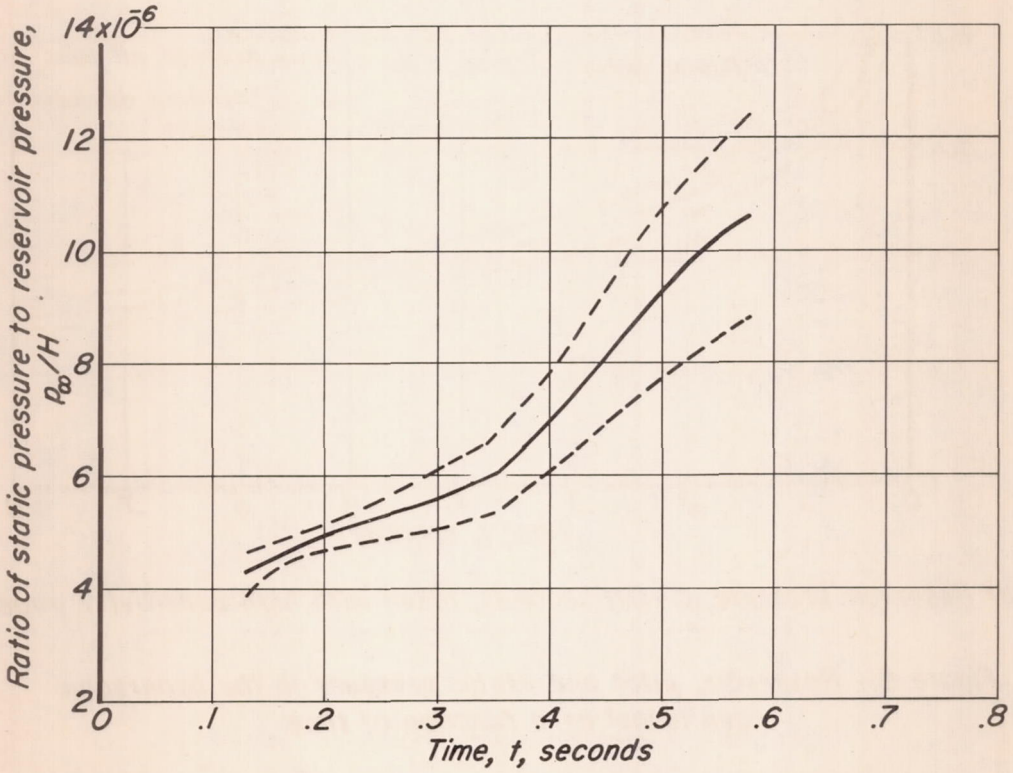

(d) Ratio of static pressure to reservoir pressure.

Figure 5.– Concluded.

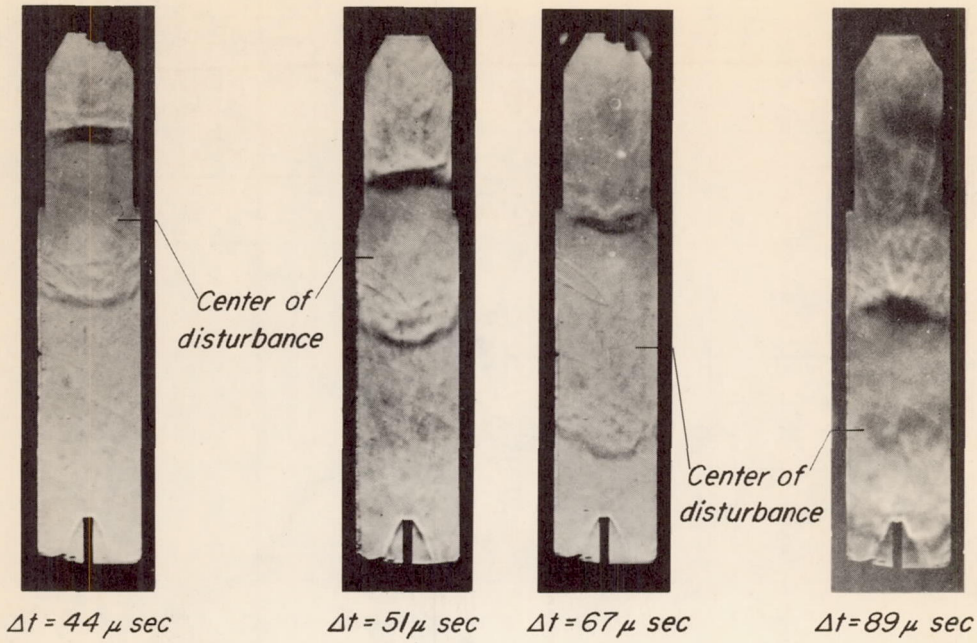

(a) Schlieren photographs of the spark discharge disturbance sweeping through the test region.

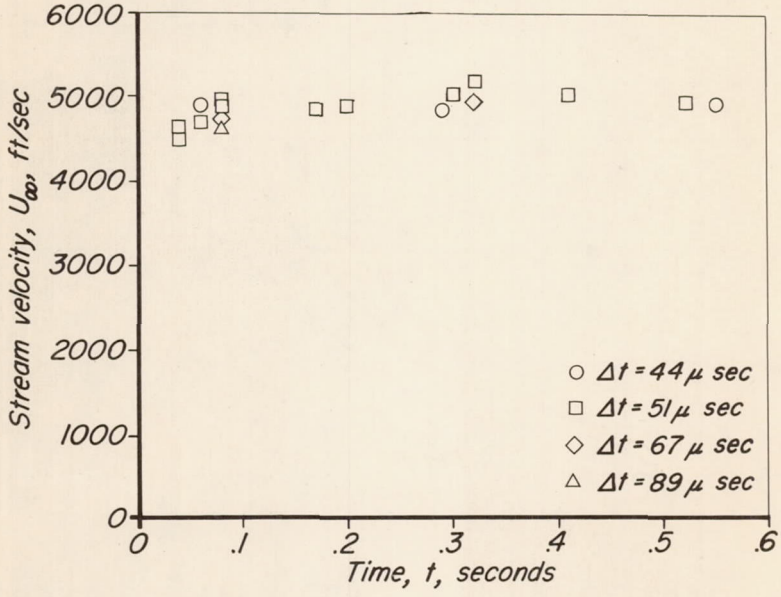

(b) Observed velocities as a function of time.

Figure 6.– Free-stream velocity as a function of time (Δt–time interval between spark discharge and Schlieren exposure, t–time of flow measured from nozzle valve opening).

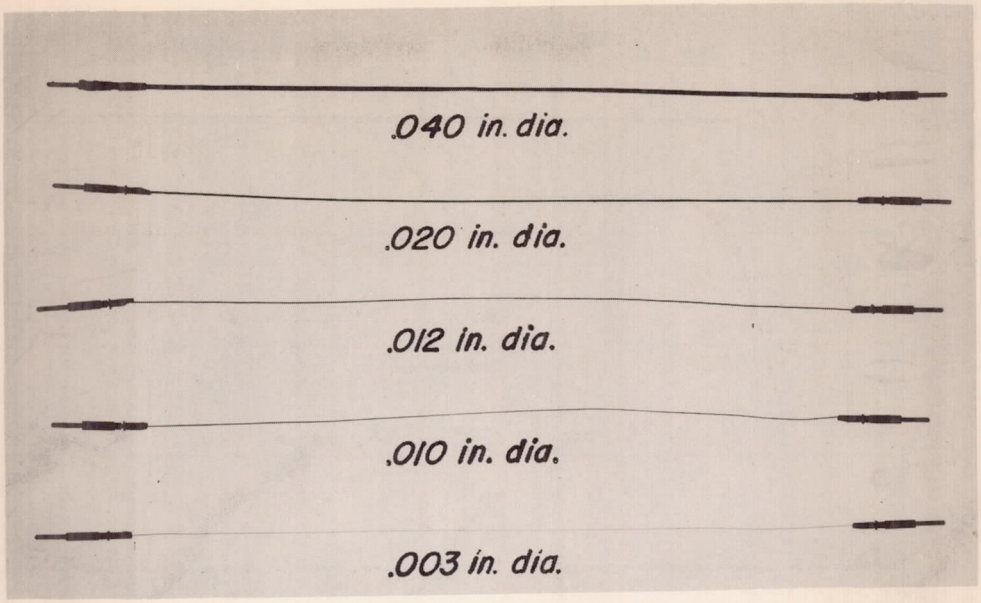

A-19938.1

(a) Thermocouple cylinders.

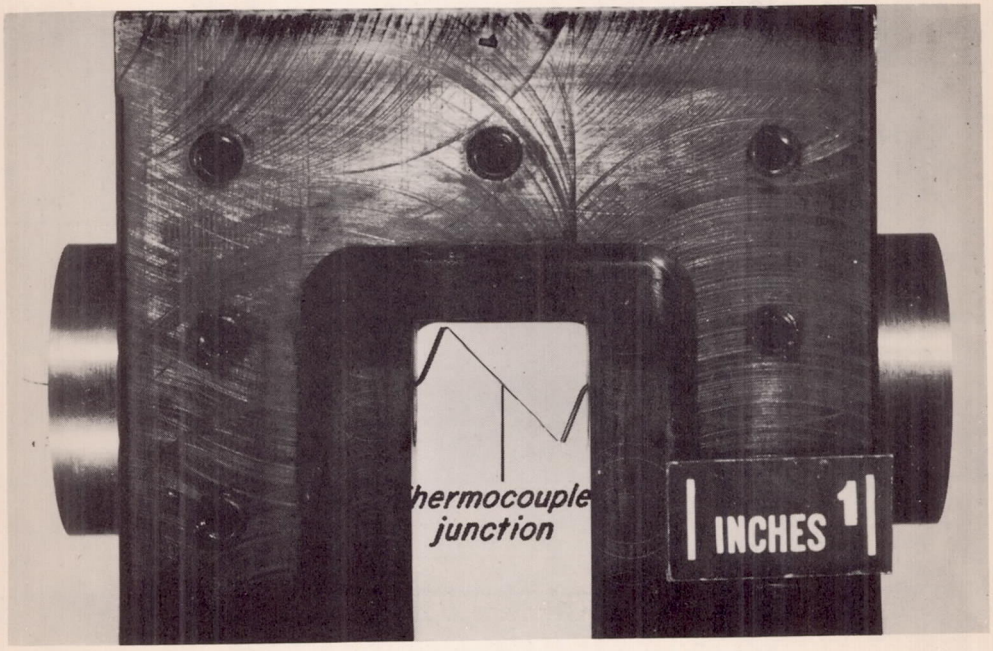

A-19917.1

(b) .020-inch-diameter thermocouple cylinder mounted in the test section at 45° yaw.

Figure 7.- Heat-transfer models.

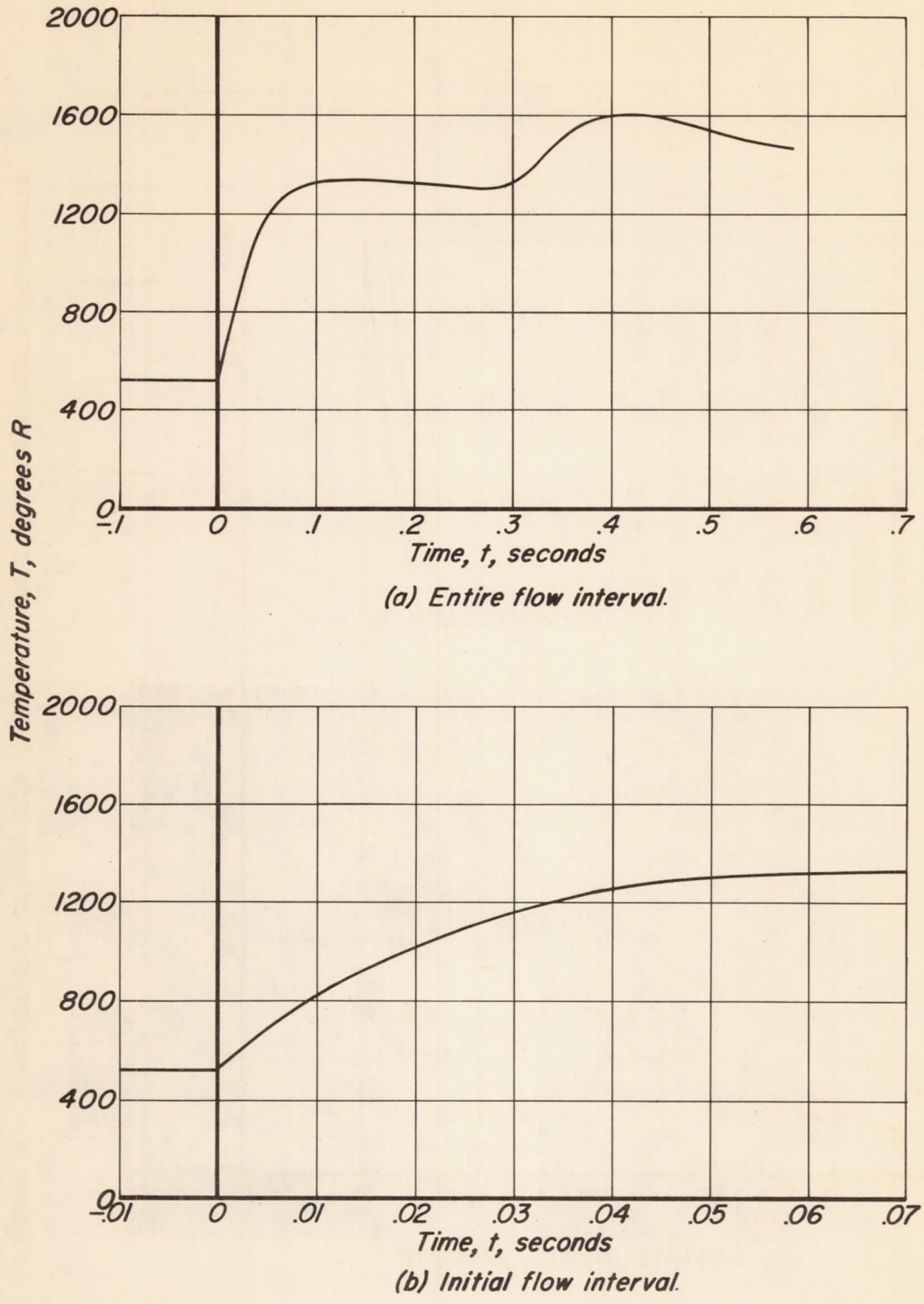

Figure 8.– Temperature of the .003–inch-diameter cylinder at zero yaw as a function of time.

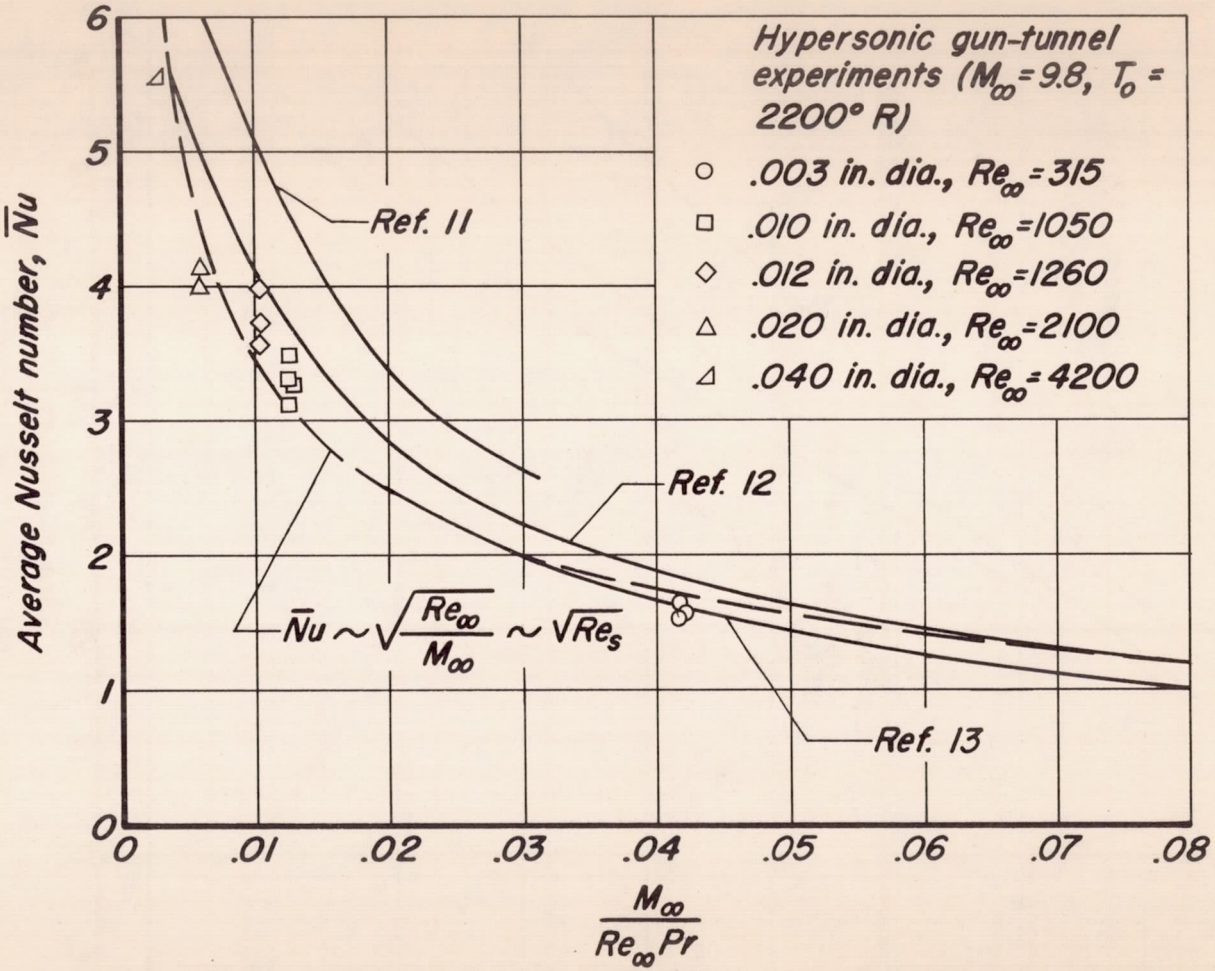

Figure 9.– Comparison of average Nusselt numbers for cylinders transverse to flow.

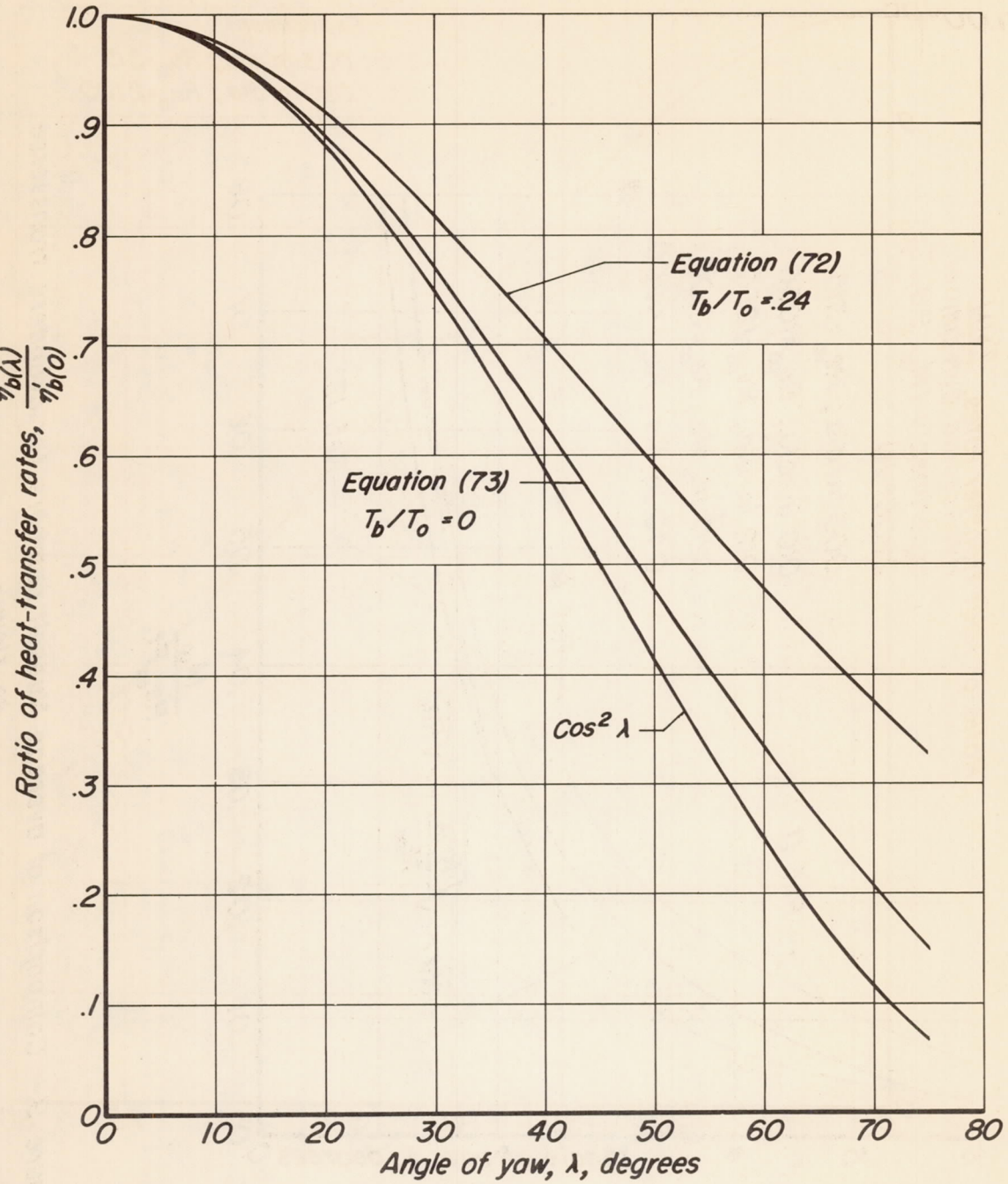

Figure 10.– Effect of yaw on heat-transfer rates to the stagnation region of a cylinder.

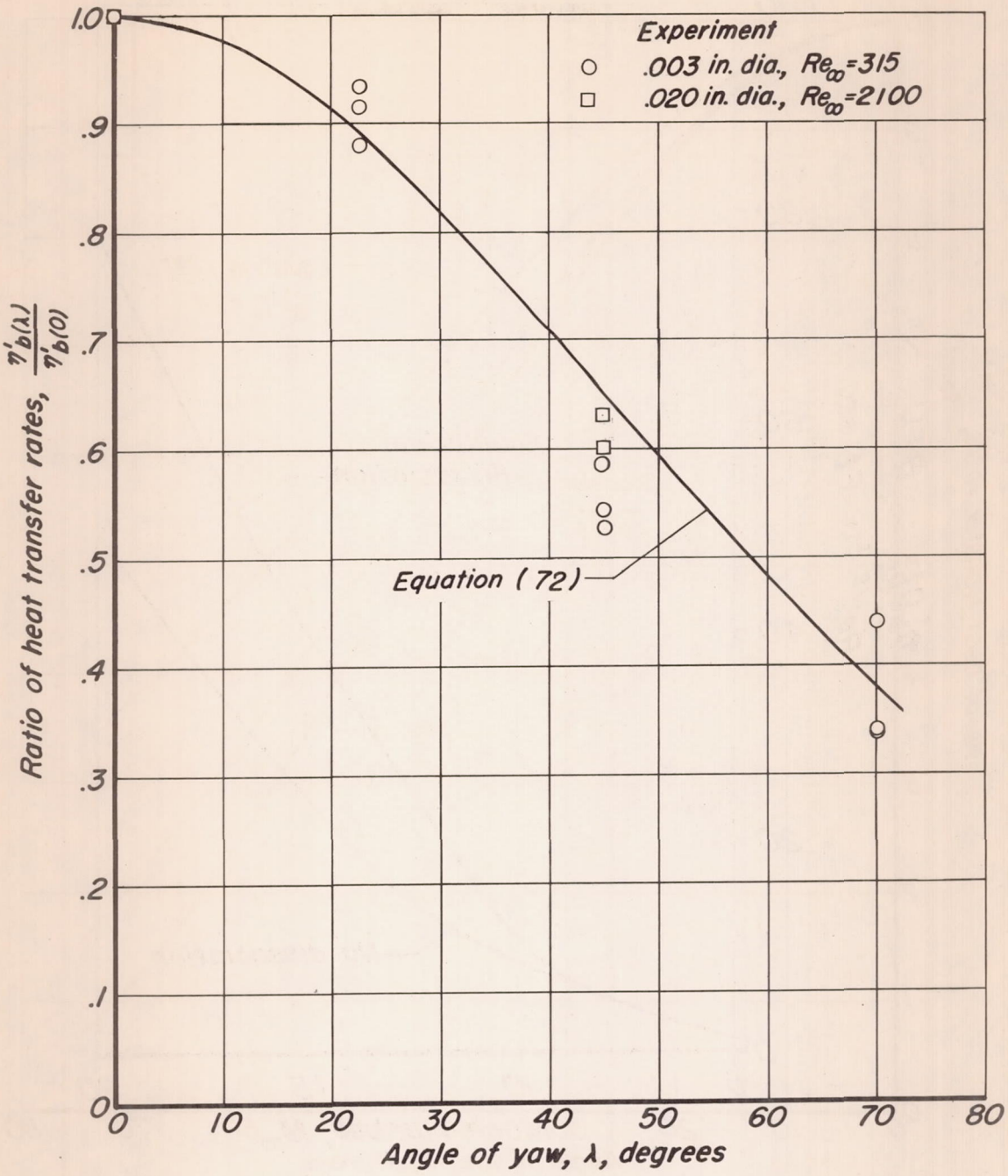

Figure 11.– Comparison of theory and experiment for the effect of yaw on the rate of heat transfer to a cylinder (M_∞=9.8, T_o =2200°R T_b/T_o = .24, Re_∞=1.26 x 10^6 per foot).

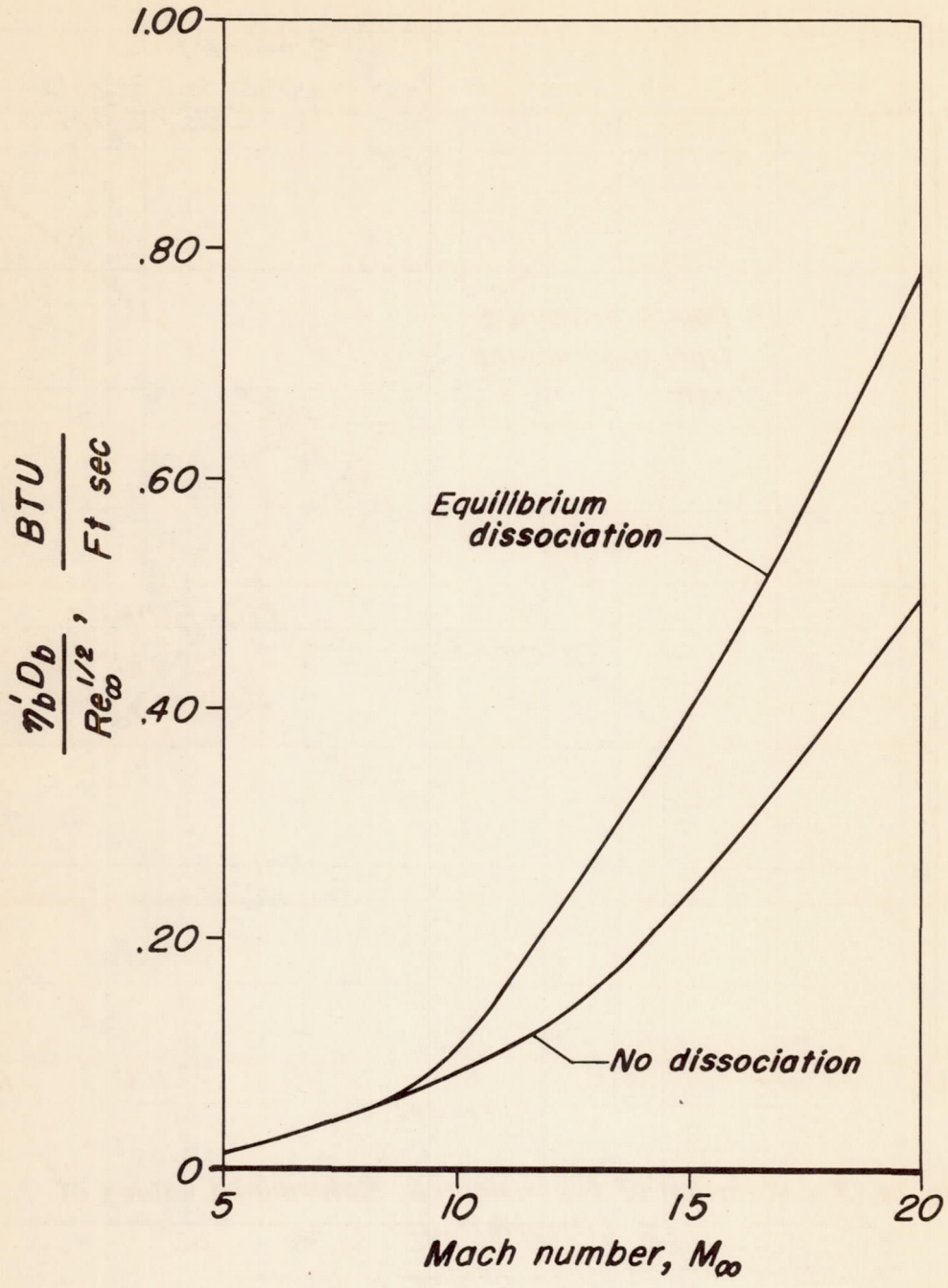

Figure 12.– Effect of equilibrium dissociation on the rate of heat transfer to the stagnation region of a cool cylindrical body (p_s = 1 atm., T_∞ = 400°R.)

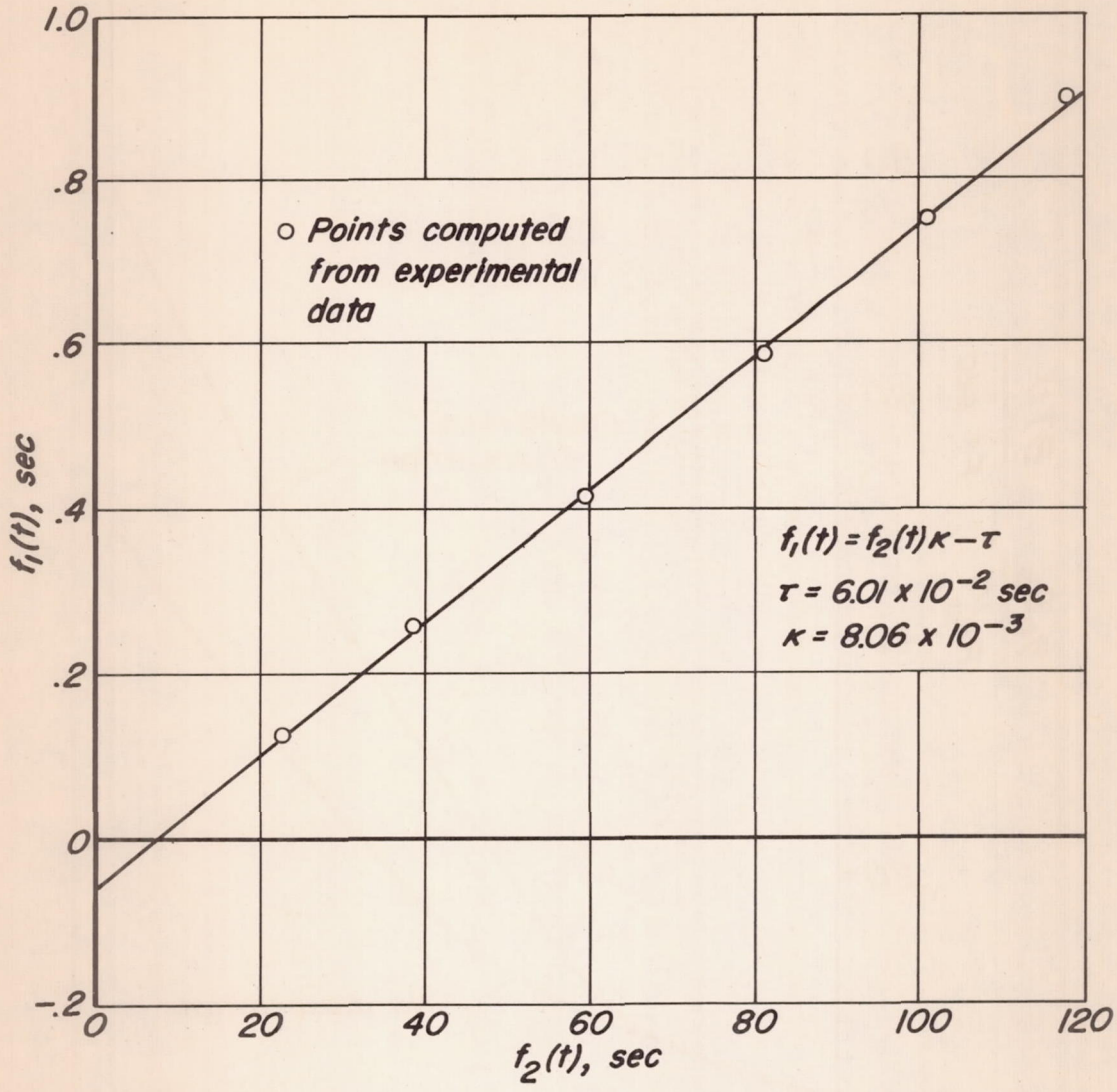

Figure 13.- Variation of experimentally determined values of $f_1(t)$ with $f_2(t)$.

NACA - Langley Field, Va.